

**THE FINE STRUCTURE OF  
DISTORTION PRODUCT OTOACOUSTIC EMISSIONS:  
THE PRIMARY ORIGIN**

**DISSERTATION**

**Presented in Partial Fulfillment of the Requirements for  
the Degree Doctor of Philosophy in the Graduate  
School of the Ohio State University**

**By**

**Yafei Du, B.M.**

**The Ohio State University  
2003**

Dissertation Committee:

Professor Lawrence L. Feth

Professor Lisa J. Stover

Professor Kamran Barin

Approved by

\_\_\_\_\_

**Advisor**

**Speech and Hearing Science  
Graduate Program**



## **ABSTRACT**

The  $2f_1-f_2$  distortion product otoacoustic emission (DPOAE) fine structure may be a more sensitive indicator of cochlear damage than DPOAE level alone. The evaluation of fine structure could considerably improve the clinical use of DPOAEs for early identification of hearing loss. However, the clinical interpretation of the DPOAE fine structure needs the clarification of the origin of the DPOAE fine structure in terms of frequency selectivity and site of lesion. Previous studies hypothesized that the DPOAE fine structure was due to the interference between the two generation sources. However, some of the data from previous studies do support an alternative hypothesis that the DPOAE fine structure is dominated by the local impedance property of the cochlear partition at the distortion product (DP) place. This study investigated this hypothesis by measuring DPOAEs and separating the  $2f_1-f_2$  DPOAE into its early and late components under different test protocols. Three findings support the hypothesis that the DPOAE fine structure is dominated by the local impedance property of the cochlear partition at the characteristic DP place. First, the  $2f_1-f_2$  DPOAE and its late component fine structure have similar fine structure pattern in terms of peak-to-peak frequency space

and peak-to-valley level difference for the same test protocol and the same test frequency range for each individual subject. Second, both early and late components of  $2f_1-f_2$  DPOAE showed smooth patterns when the  $f_{dp}$  was held constant. This indicates that when the characteristic DP place along the cochlear partition was held constant across the test frequency range, the DPOAE late components are generated at the same place and minima and maxima were not observed. The phase of the late component still showed rapid changes due to forward traveling wave moving along the cochlear partition when  $f_{dp}$  was held constant. No late component fine structure was obtained in despite of an existing interference between the two generation sources. Third, the  $2f_1-f_2$  DPOAE late components obtained from the same characteristic DP frequency range under different test protocols showed a similar pattern of DPOAE fine structure in terms of the peak-to-peak frequency space and peak-to-valley level difference despite the interference between the two DPOAE generation sources. The data obtained from this study support the hypothesis that the impedance property of the cochlear partition at the particular characteristic  $f_{dp}$  place dominates the DPOAE fine structure rather than the interference between the two DPOAE generation sources. The existing of the DPOAE fine structure depends on the anatomical function of the particular portion of cochlear partition. Lack of the DPOAE fine structure may indicate a damage of the cochlear partition at particular DP place.

**Dedicated to my father and mother**

## **ACKNOWLEDGMENTS**

I wish to thank my adviser, Dr. Lisa J. Stover, and Dr. Lawrence L. Feth, for intellectual support, encouragement, and enthusiasm which made this dissertation possible, and for their patience in correcting my stylistic, scientific and language errors.

I thank Dr. Kamran Barin for serving as my dissertation committee member and for providing valuable scientific suggestions.

I also wish to thank John Zimmer for helping me to handle various computer problems and transfer out my data from the old computer.

## VITA

March 6, 1961..... Born-Beijing, China

1984.....B. Medicine, Beijing Medical University

1984-1994.....Doctor,

Beijing Peoples Hospital, Beijing China

1995-1998.....Researcher

Beijing Long Xing Technology Ltd. Inc.

1998-present.....Graduate Research Associate,

The Ohio State University

## PUBLICATIONS

- 1, Du Y (1987) Measurement of mycetric temperature and pH of children aged 10-12 in urban and suburban Beijing; *Chinese Journal of Otorhinolaryngology*
- 2, Du Y (1987) Treating laryngostenosis with Co2 laser; *Foreign Medicine*

- 3, Du Y (1990) Case report: The ala nasi recreated from auricular cartilage; *Beijing Medical University Press*
- 4, Du Y (1992) Case report: Cholesteatomatous otitis media supervention with tubercular meningitis; *Wuhan Journal of Clinical Otolaryngology*
- 5, Du Y (1993) Clinical analysis of 302 cases of nasal endoscopy examination; *Beijing Medical University Press*

### **FIELDS OF STUDY**

Major Field: Speech and Hearing Science

## TABLE OF CONTENTS

	Pages
Abstract.....	ii
Dedication.....	iv
Acknowledgement.....	v
Vita.....	vi
List of Tables.....	x
List of Figures.....	xi
Chapters	
1. Introduction and literature review.....	1
1.1. Cochlear mechanism.....	1
1.2 Distortion product otoacoustic emissions (DPOAEs).....	5
1.3 Primary and secondary sources.....	11
1.4 Interaction between two sources.....	18
2. Methodology.....	26
2.1. Subject.....	26
2.2. Stimuli.....	26
2.3. Testing protocols.....	27
2.4. Data collection.....	30
2.5. Data analysis.....	30

3. Results.....	35
3.1. Data replication .....	35
3.2. Fine structure.....	35
3.3. $2f_1-f_2$ DPOAE early and late components.....	43
3.4. Comparisons.....	49
3.5. Phase.....	60
4. Discussion.....	66
4.1. Fine structure.....	66
4.2. Early and late components.....	67
4.3. Comparisons.....	70
4.4. Phase.....	73
4.5. Further research and limitations of this study.....	73
5. Conclusion.....	79
Appendix A MatLab program for calculating the amplitude of DPOAEs.....	80
Appendix B MabLab program for separate the DPOAE early and late components..	81
Appendix C MabLab program for phase unwrapping .....	83
Bibliography.....	85

## LIST OF TABLES

<u>Tables</u>	<u>Pages</u>
1. Summary of five DPOAE data collection protocols for this experiment.....	29
2. The fine structure index of the $2f_1-f_2$ DPOAE fine structures for the fixed $f_2/f_1$ ratio, the fixed $f_2$ , the $f_1$ fixed at 3000 Hz and the $f_1$ fixed at 2800 Hz protocols, for all five subjects.....	43
3. The fine structure index of $2f_1-f_2$ DPOAE late components for the fixed $f_2/f_1$ ratio, the fixed $f_2$ , the $f_1$ fixed at 3000 Hz and the $f_1$ fixed at 2800 Hz protocols for all five subjects.....	49
4. The width of ripples which are caused by the rectangular gate function for each test protocol and each subject.....	76
5. The comparison of the width of ripples insignal processing and width of notch in $2f_1-f_2$ DPOAE Amplitude curve which occurred in each of protocols for each subjects .....	76

## LIST OF FIGURES

Figures	Page
1. Illustration of the theoretical behavior of the amplitude of distortion as frequency $f_1$ is removed from frequency $f_2$ . .....	10
2. Illustration of the various steps of data processing. ....	31
3. Illustration of the measurement of DPOAE fine structure index. ....	34
4. Illustration of the replicability of amplitude of $2f_1-f_2$ DPOAE using the fixed $f_2/f_1$ ratio protocol. ....	36
5. The amplitude of $2f_1-f_2$ DPOAE using the fixed $f_2/f_1$ ratio protocol.....	37
6. The amplitude of $2f_1-f_2$ DPOAE using the fixed $f_2$ Hz protocol.....	38
7. The amplitude of $2f_1-f_2$ DPOAE using the $f_1$ fixed at 3000 Hz protocol.....	39
8. The amplitude of $2f_1-f_2$ DPOAE using the $f_1$ fixed at 2800 Hz protocol.....	40
9. The amplitude of $2f_1-f_2$ DPOAE using the fixed $f_{dp}$ protocol.....	41
10. The amplitude of separated early and later components using the fixed $f_2/f_1$ ratio protocol .....	44
11. The amplitude of separated early and later components using the fixed $f_2$ protocol .....	45
12. The amplitude of separated early and later components using the $f_1$ fixed at 3000 Hz protocol .....	46
13. The amplitude of separated early and later components using the $f_1$ fixed at 2800 Hz protocol.....	47
14. The amplitude of separated early and later components using the fixed $f_{dp}$ protocol.....	48
15. The amplitude of $2f_1-f_2$ and its late component using the fixed $f_2/f_1$ ratio protocol.....	50
16. The amplitude of $2f_1-f_2$ and its late component using the fixed $f_2$ protocol.....	51
17. The amplitude of $2f_1-f_2$ and its late component using the $f_1$ fixed at 3000 Hz protocol.....	52
18. The amplitude of $2f_1-f_2$ and its late component using the $f_1$ fixed at 2800 Hz protocol.....	53
19. The amplitude of $2f_1-f_2$ and its late component using the fixed $f_{dp}$ protocol.....	54
20. The comparison of $2f_1-f_2$ DPOAE early components between the fixed $f_2/f_1$ ratio and $f_1$ fixed at 2800 Hz protocols.....	56
21. The comparison of $2f_1-f_2$ DPOAE early components between the fixed $f_2/f_1$ ratio and fixed $f_{dp}$ protocols.....	57
22. The comparison of $2f_1-f_2$ DPOAE late components between the fixed $f_2/f_1$ ratio and fixed $f_2$ protocols.....	58

23.	The comparison of $2f_1-f_2$ DPOAE early components between the fixed $f_2/f_1$ ratio and $f_1$ fixed at 3000 Hz protocols.....	59
24.	The phase of $2f_1-f_2$ DPOAE early and late components using the fixed $f_2/f_1$ ratio protocol.....	61
25.	The phase of $2f_1-f_2$ DPOAE early and late components using the fixed $f_2$ protocol.....	62
26.	The phase of $2f_1-f_2$ DPOAE early and late components using the $f_1$ fixed at 3000 Hz protocol.....	63
27.	The phase of $2f_1-f_2$ DPOAE early and late components using the $f_1$ fixed at 2800 Hz protocol.....	64
28.	The phase of $2f_1-f_2$ DPOAE early and late components using the fixed $f_{dp}$ protocol.....	65

## **CHAPTER 1**

### **INTRODUCTION AND LITERATURE REVIEW**

#### 1.1. Cochlear mechanisms

The human peripheral auditory system includes three major parts: the outer ear, the middle ear, and the inner ear. The outer and middle ears serve as protective, conductive, and filtering devices. The cochlea (part of the inner ear) is a long, tapered cavity in the temporal bone, which is filled with fluid. The cavity is coiled into a tight spiral. The broad end close to the middle ear is called the base. The narrow end of the spiral is the apex. This fluid space is divided lengthwise into three compartments, called scala media, scala vestibuli, and scala tympani.

The main task of the mammalian cochlea is to analyze sound in terms of its intensity, timing, and frequency content. The cochlea is a complex hydromechanical system activated by the motion of the stapes footplate. The basilar membrane, which separates the scala media from the scala tympani, is composed mainly of extracellular matrix material, with fibers embedded in a homogeneous ground substance. Two structures sit on the basilar membrane in scala media, the sensory epithelium known as the organ of Corti and a gelatinous structure called the tectorial

membrane. These three elements, basilar membrane, organ of Corti, and tectorial membrane, collectively known as the cochlear partition, are directly responsible for sensory function in the cochlea. The structure of the basilar membrane contributes to the stiffness and mass of the cochlear partition. In the normal human adult, the stiffness decreases progressively towards the apex while the mass increases. In the base of the cochlea the basilar membrane is narrow and thin, progressing to the apex where it is wider and thicker. The vibration of the cochlear partition normally takes the form of waves or ripples that travel away from the stapes and toward the cochlear apex, but do not travel the entire length of the cochlear partition. For a pure-tone stimulus, the wave grows as it travels, reaching a maximum at a position known as the wave's characteristic place, and then collapses abruptly so that no vibration exists beyond a cochlear position known as the wave's cutoff region just apical to the characteristic place. The characteristic place and cutoff region are positioned along the cochlear length according to a place-frequency map: high frequencies toward the base and low frequencies close to the apex.

The organ of Corti, containing both sensory and supporting cells on the basilar membrane. It is loosely structured to permit movement of the sensory epithelium in response to mechanical stimuli, yet it is rigid enough to transmit vibrations from the basilar membrane to the stereocilia, which located on the top of each hair cell. The arrangement and structure of sensory and supporting cells confer the primary structure of the organ of Corti and its principal mechanical properties. There are two types of sensory cells, inner hair cells (IHCs) and outer hair cells (OHCs). Inner hair

cells play a primarily sensory role in the cochlea, based on the fact that most of the afferent nerve fibers synapse with them. Outer hair cells, although providing some direct sensory input to the central nervous system, more likely modify the mechanical properties of the cochlea and the basilar membrane.

A stimulus consisting of two frequency components  $f_1$  and  $f_2$  ( $f_1 < f_2$ ) often gives rise to tones with frequencies that do not correspond to  $f_1$  and  $f_2$  but to frequencies such as  $2f_1 - f_2$ ,  $3f_1 - 2f_2$ ,  $2f_2 - f_1$  etc. These tones were called combination tones in the 1960's and 1970's. They are now more commonly called distortion products.

These distortion products can be heard and measured psychoacoustically (Goldstein, 1967; Smoorenburg, 1972). The main features of these distortion product tones are that they can be perceived at low stimulus levels as long as the higher frequency stimulus ( $f_2$ ) exceeds the hearing threshold and that they are perceived only in a restricted frequency region below  $f_1$  and for small frequency differences between the two stimulus components (Smoorenburg, 1972). When the level of the two primary stimuli increases, distortion product levels increase almost in direct proportion to primary-tone levels (Wilson, 1980).

The perception of these distortion product tones at low stimulus intensities suggests the presence of significant nonlinearities in the cochlea, which can be best explained by an active process requiring energy. These nonlinearities only exist in a live, healthy cochlea. The observations of basilar membrane motion in the living

cochlea (Rhode, 1971; Davis, 1983; Ruggero and Rich, 1991) revealed that the basilar membrane is tuned just as sharply as hair cells and auditory nerve fibers. Therefore, the cochlear amplifier must be located in the basilar membrane complex itself. This has led to the suggestion that an active process exists, requires energy and is located between the basilar membrane and the auditory nerve fiber, that is, at the outer hair cells.

Outer hair cells have active properties that increase mechanical energy within the cochlea, increasing stimulus-specific vibrations of the basilar membrane. This energy is transmitted to the inner hair cells and enhances hearing sensitivity and frequency selectivity. How the mechanical responses of individual outer hair cells interact with the motion of the cochlear partition is not yet clear. However, the outer hair cells are interconnected by the cytoarchitecture of the organ of Corti; thus, if many cells move in synchrony their mechanical response can sum. Measurement of the force generated by individual outer hair cells indicate that the activation of large numbers of cells in concert should be able to change the mechanical responses of the cochlear partition (Iwasa & Chadwick, 1992). One result of this is thought to be amplification of basilar membrane motion in a narrow frequency range. Thus, the action of outer hair cells has been referred to as the 'cochlear amplifier'. The implication is that outer hair cells by themselves can induce basilar membrane motion, which can be indirectly measured in the ear canal as otoacoustic emissions.

## 1.2. Distortion product otoacoustic emissions (DPOAEs)

Distortion product otoacoustic emissions (DPOAEs) are sounds recorded in the ear canal which are generated in the cochlea (Kemp, 1979). They are produced through the nonlinear interaction of two closely spaced, external primary tones of frequencies  $f_1$  and  $f_2$  with  $f_2$  greater than  $f_1$ . When the normal ear is stimulated simultaneously by two primary tones ( $f_1$  and  $f_2$ ), low-level, intermodulation distortion products (DP) can be measured in the ear canal. They may appear at frequencies equal to  $2f_1 - f_2$ ,  $3f_1 - 2f_2$ ,  $4f_1 - 3f_2$  (lower-sideband distortion products), and  $2f_2 - f_1$ ,  $3f_2 - 2f_1$  (higher-sideband distortion products) etc.

By definition, DPOAEs represent evoked nonlinear responses, because they consist of new frequencies that are not present in the eliciting stimuli (Kemp, 1979). This distortion is a by-product of the amplification process of the outer hair cell active mechanism. In ears damaged by exposure to extremely high levels of noise, or ototoxic drugs, DPOAEs are eliminated or reduced in amplitude. Histological examination has revealed that outer hair cell damage is the anatomical correlate to the reduction of DPOAE levels, thus verifying the involvement of outer hair cells in the generation of otoacoustic distortion (Brown, McDowell, and Forge, 1989).

The amount of distortion, and thus the amplitude of the DPOAEs, is dependent on several parameters of the primary stimuli, the overall health of the cochlea, and irregularity in the characteristic impedance along the cochlear partition. The amplitude of DPOAEs depends on the level ( $L_1$ ,  $L_2$ ) and frequency ( $f_1$ , and  $f_2$ ) of the

primaries, their frequency separation or ratio ( $f_2/f_1$ ), and their relative levels ( $L_1-L_2$ ). In humans, DPOAE amplitude is usually about 40 to 50 dB lower than that of primary-tone levels (Brown & Kemp, 1984; Harris, Lonsbury-Martin, Stager, Coats, and Martin, 1989). However, through enhancement by the presence of spontaneous otoacoustic emission (SOAE) in the same narrow frequency range of DPOAEs, the amplitude of DPOAEs can reach unusual levels that might be only 10 to 20 dB less than those of the primaries (Kemp & Brown, 1984).

Generally, DPOAE amplitude is higher for  $f_2$  in the region from 2000 Hz to 4000 Hz. Lower DP levels for  $f_2$  below 2000 Hz are in general agreement with other observations of reduced amplification in the apical regions of the cochlea, but may also be due to measurement difficulties. Above 4000 Hz, there are measurement issues as well, although not due to biological noise as in the case of lower frequencies, but rather due to reduced wavelengths and standing waves in the outer ear canal (Probst and Lonsbury, 1990).

With DPOAE's 40 to 50 dB below primary-tone levels, it becomes more difficult to measure them when the primary levels drop below 40 dB SPL. The relationship of stimulus intensity level to DPOAE amplitude is demonstrated by the DPOAE input-output (I/O) function. A DPOAE I/O function can be obtained when the stimulus frequencies are held constant while stimulus intensity is either increased from a low level or decreased from a high level. The DPOAE I/O function does not always show a monotonic shape as the stimulus intensity increases. DPOAE

amplitude growth begins slowly at low stimulus intensity levels and increases more steeply for moderate to high stimulus intensities. However, DPOAE amplitude saturates at stimulus levels in the range of 65 to 75 dB SPL. As with frequency, the relative level of the primaries is also important. Empirical data indicated that non-monotonicities in I/O functions are minimized when  $L_2$  is less than  $L_1$ . This condition maximizes primary interaction without over-driving the  $f_2$  place. The DPOAE amplitude is most robust when  $L_1$  is 10 dB higher than  $L_2$  with  $L_1$  approximately 65 dB (Stover, Gorga, Neely, 1996).

The frequency separation between the two primaries is also crucially important. The relative frequency or the ratio of the higher ( $f_2$ ) to lower ( $f_1$ ) primary frequency ( $f_2/f_1$  ratio) defines the separation between the two primary frequencies. A DPOAE will not be generated if these two primary frequencies are too far apart (e.g.  $f_2/f_1$  ratio greater than 1.5) or too close together (e.g.  $f_2/f_1$  ratio less than 1.01). Wilson (1980) demonstrated that the largest amplitudes occur with  $f_2/f_1$  ratios between 1.1 and 1.2. DPOAE levels exhibit a bandpass shape, a filterlike property having low- and high-frequency slopes, when the frequency of either primary is varied (Gaskill & Brown 1990, Harris, Lonsbury-Martin, Stager, Coats, and Martin 1989). If one holds  $f_2$  constant and varies  $f_1$ , then the DPOAE will reach maximum absolute amplitude when the distortion product ( $f_{dp}$ ) occurs in a frequency region approximately  $\frac{1}{2}$  octave below  $f_2$  (i.e., when the  $f_2/f_1$  ratio is 1.2 to 1.25), and decreases as  $f_1$  either approaches or further separates from  $f_2$  (Gaskill & Brown 1990). Similar bandpass shapes in DPOAE amplitude also have been found when  $f_1$

is held constant and  $f_2$  is swept or if  $f_{dp}$  is held constant and both primary frequencies are changed. Initially at low  $f_2/f_1$  ratio settings, DPOAE amplitude will be at a minimum. Then as  $f_1$  and  $f_2$  are separated further, the amplitude of the DPOAE increases until a maximum is reached. Finally, DPOAE levels undergo another systematic decrease as separation of the primary tones continues until DPOAEs are indistinguishable from the noise floor (Harris et al. 1989). The noise floor is defined as the amplitude of background noise that occurs at or near the test frequency at the time of recording.

Finally, DPOAE levels are influenced idiosyncratically by random fluctuations in the characteristic impedance of the cochlear partition. Peaks and valleys in the amplitude of frequency-contiguous distortion product otoacoustic emissions are collectively called DPOAE fine structure or DPOAE microstructure. DPOAE fine structure has been described by several investigators using either moving stimuli at a fixed  $f_2/f_1$  ratio (Gaskill and Brown, 1990; He and Schmiedt, 1993) or with one stimulus fixed and a varied  $f_2/f_1$  ratio (Harris et al., 1989; Gaskill and Brown, 1990; Harris and Brown, 1994). In both paradigms, the periodicity of the fine structure is proportional to frequency and is about the same as that seen in the response to a swept single tone, which is known as the stimulus frequency otoacoustic emission (SFOAE). The same fine structure also can be seen in auditory thresholds (Kemp, 1979; Schloth, 1983; Long, 1984; Harris and Brown, 1994). The pattern of DPOAE fine structure can be quite different from subject to subject. The individual patterns are repeatable across sessions at the same primary levels. The fine structure has a

frequency spacing of about 0.094 (3/32) octave between neighboring peaks or valleys, and peak-to-valley level differences up to 20 dB and, by definition, no less than 3 dB. The fine structure is less pronounced at frequencies above 4000 Hz. The DPOAE fine structure pattern shifts downward in frequency with increasing primary level (He and Schmiedt, 1993).

Theoretically, distortion is proportional to the displacement of the basilar membrane distributed around the point of maximal interaction between the two primaries, which occurs in the cutoff region of  $f_2$ . This distortion originates in the shearing force on the stereocilia of the outer hair cells (Kemp, 1979). Figure 1 illustrates that for a given  $f_2$  place, the distortion generated would decrease in amplitude monotonically as  $f_1$  is moved away from  $f_2$ . This distortion propagates to the  $f_{dp}$  place and generates a neural response that leads to psychophysically measured distortion. As this theory would predict, the psychophysical measured distortion also monotonically decreases in amplitude as the  $f_2/f_1$  ratio is increased. However, as described above, DPOAEs demonstrate a bandpass characteristic as opposed to the low pass behavior of their psychophysical measurement. The bandpass characteristic of DPOAEs is difficult to explain in terms of a single distortion product otoacoustic emission generation source at  $f_2$  place. Thus there must be some secondary mechanism operating in the generation of the acoustic manifestation of this intermodulation distortion.

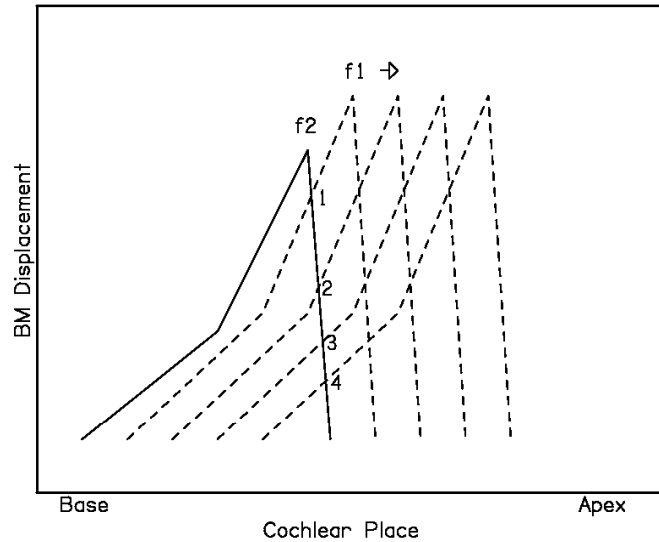


**Figure 1: Illustration of the theoretical behavior of the amplitude of distortion as frequency  $f_1$  is moved away from frequency  $f_2$ . As the primaries are separated, the point of maximum overlap of two primary traveling wave envelopes (indicated by the numbers 1-4) occurs at lower and lower amplitudes.**

In summary, distortion product otoacoustic emissions are intermodulation distortion products caused by the basilar membrane's nonlinear response to a two-tone stimulus, which occurs near the  $f_2$  place. However a model with only one generation source at the  $f_2$  place does not explain the DPOAE fine structure and the bandpass characteristic of DPOAEs. It is still a point of debate whether one or multiple generation-sources contribute to DPOAEs. With so many degrees of freedom in the stimulus space, and the lack of a comprehensive model of distortion generation, clinical interpretation of DPOAE is difficult, at best.

### 1.3. Primary and secondary sources

Although the generation of distortion products due to the interaction of the two primaries is, in principle, spread over the whole cochlea, a region of about 1mm around the characteristic place of  $f_2$  has been suggested as the major contributor of the DPOAE. This can be demonstrated by adding a suppressor tone between  $f_1$  and  $f_2$ , which effectively diminishes the DPOAE emission amplitude (Brown & Kemp 1983). This emission generation site at the region of maximum overlap of the two traveling wave envelopes evoked by the two primaries is referred to as the  $f_2$  site.

There still are some arguments about whether only one distortion product otoacoustic emission generation source or multiple generation sources contribute to DPOAEs. Since the DPOAE recorded in the ear canal consist of new frequencies ( $f_{dp}$ ) that are not present in the eliciting stimuli, it seems clear that there is at least one more energy source at the  $f_{dp}$  characteristic place, in the form of the stimulus frequency emission (Brown and Gaskill, 1990; Gaskill and Brown, 1996; Stover, Neely, and Gorga, 1996). Recent studies have indicated this second source contributing to the lower-sideband distortion product otoacoustic emissions ( $2f_1-f_2$ ,  $3f_1-2f_2$ ,  $4f_1-3f_2$ , etc.). Some studies demonstrated this primary- and secondary-source hypothesis by introducing a third tone with low intensity close to the distortion product frequency ( $f_{dp}$ ) as a suppressor (Gaskill and Brown 1996). With increasing suppressor level, the DPOAE level showed an initial small suppression with a relative stable plateau or gradual decline, followed by a rapid decline. Gaskill &

Brown (1996) explained that at lower suppressor levels, the DPOAE generation source at the  $f_{dp}$  place is affected. Then, as the intensity level of the suppressor tone increases, suppression of the generation source at  $f_2$  place begins and DPOAE level rapidly declines.

Heitmann, Waldmann, and Schnitzler (1998) indicated that the suppression of distortion product otoacoustic emissions near the  $f_{dp}$  place showed a three-step behavior. For low suppressor levels, the emission either decreased or increased when increasing the suppressor. This step depends on the DPOAE fine structure; if the DP is at a peak, the DPOAE is reduced; but if the DP is at a valley, the DPOAE is increased. The low-level suppressor leads to a locally restricted excitation pattern on the basilar membrane; this will suppress the secondary generation source at the  $f_{dp}$  place, leaving only the response from the primary generation source at the  $f_2$  place to be recorded in the external ear canal. For intermediate suppressor levels, DPOAE amplitude was constant and independent of suppressor level. In this step, since the DPOAE fine structure has already been removed, the suppressor can have no further effect at the  $2f_1-f_2$  place but will be too weak to influence the distant primary generation source at the  $f_2$  place. For high suppressor levels, the DPOAE always decreased with further increase of the suppressor. At this step, the suppressor tone affects the primary generation source near the  $f_2$  place due to its wider traveling wave envelope, which extends to the  $f_2$  site.

Stover, Neely, and Gorga (1996) tested the two-source hypothesis using the latency of the DPOAE, which has been argued to be an indirect measurement of the site of generation. Theoretically, the response latency should represent the sum of forward travel time of the stimulus to the generation site and the reverse travel time as the OAE travels from this site back out of the cochlea, through the middle ear to the ear canal. Because the two sites are spatially separated, backward-traveling waves generated at the more apical location (the  $2f_1-f_2$  site) must travel further to reach the ear canal than the waves generated at the basal location (the  $f_2$  site). Consequently, waves from the apical site are delayed relative to the basal site. Stover et al. (1996) measured DPOAEs with fixed  $f_2$  and swept  $f_1$ , across a wide range of primary levels. They observed a complex latency structure with multiple peaks in the envelope of the time waveform. The latency of individual peaks remained constant across levels; however, short latency peaks had the greatest amplitudes at higher levels, and longer latency peaks are largest at low levels. The short latency peaks had a higher threshold, with rapid growth and little or no saturation. Later occurring peaks were present with lower level stimulation but amplitude growth is more gradual and perhaps saturates at higher levels of stimulation. These results are consistent with the idea that there are multiple generation sources which contribute to DPOAEs. There is one source corresponding to the shortest latency peak, and later occurring events are the result of at least one other source and possibly interactions between the multiple sources.

According to the two-source hypothesis, the primary source is the nonlinear interaction between the two primaries at the initial generation site close to the  $f_2$  place. This part of the DPOAE has been termed “wave-fixed” because it moves with the traveling wave as frequency changes. The secondary source is at the characteristic site of the particular DP frequency, and results from a linear reflection of the forward-traveling wave off “random” perturbations in mechanics of the cochlea, the same as the stimulus frequency emission. This component of the DPOAE is called “place-fixed” because the fixed perturbation place responds to different phases of the stimulus as its frequency changes.

Kemp (1983) first defined the term “wave-fixed” and “place-fixed”. Theoretically, loss of traveling wave energy through viscous forces is inevitable in a structure like the organ of the Corti. Kemp (1983) indicated in his study that the outer hair cell mechanisms act to reduce mechanical energy loss and damping, and possibly to provide amplification. A sharp mechanical impulse, from outer hair cells on each cycle of excitatory displacement, would be sufficient to cancel some viscous losses and improve cochlear performance. Both loss reduction and amplification involve the conversion of metabolic energy into vibratory energy and increase a vibration at the peak of the traveling wave, but amplification only occurs when the traveling wave energy flows out of the cochlear partition. The initiation of retrograde energy transmission in the cochlea (necessary for OAEs) implies some form of localized perturbation of the ‘ideal’ forward traveling wave. Perturbation of the ‘ideal’ traveling wave would occur spatially if the normal gradation of physical

propagation characteristics were irregular. In this case, the fixed perturbation place would respond to different phases of the stimulus as its frequency was changed. This would result in emission latency twice that of the forward traveling wave up to the fixed perturbation place. This appears to be the dominant cause of stimulus re-emission in the human ear. This mechanism is called the “place-fixed”. Alternatively, mechanical nonlinearity might modify propagation conditions at the peak of response. In this case, the place of re-emission moves with the traveling wave as frequency is changed. There is little phase change and short latency. Very short latency indicates a very basal source or one created by the swept frequency traveling wave itself. This mechanism is called “wave-fixed”.

The nonlinear distortion generated at the  $f_2$  place occurs at the point of maximum overlap of the traveling wave envelopes of the two primaries. This generator moves smoothly with the  $f_2$  traveling wave as  $f_2$  is swept in frequency, and is associated with a short latency and a phase, which varies minimally. This underlying mechanism is “wave-fixed” because it moves with traveling wave as frequency changes. The linear reflection at the  $f_{dp}$  place occurs in a fixed position along the cochlear partition at the particular DP frequency place. A longer latency would be recorded and its phase would change rapidly as  $f_{dp}$  is swept along the cochlear partition. This underlying mechanism is “place-fixed”. The fixed perturbation place responds to different phases of the stimulus as its frequency changes (Kalluri and Shera, 2001). Since the emission generated at the  $f_2$  place has a shorter latency, it is known as the early component of the lower-sideband DPOAEs.

Because the emission generated at the  $f_{dp}$  place has a longer latency, it is known as the late component of the lower-sideband DPOAEs. Computer modeling by Mauermann, Uppenkamp, van Hengel, and Kollmeier (1999) showed that the component from the  $f_{dp}$  site is sensitive to the existence of fluctuations of stiffness along the cochlea partition, which are sufficient to create quasiperiodic OAE fine structure patterns, while the initial generation component is not.

Kalluri & Shera (2000) tested the key predictions of the “two-mechanism model” for the generation of distortion product otoacoustic emissions by separating the two generation sources. They used two different methods, selective suppression and spectral smoothing. The two-mechanism model predicts that the lower-sideband distortion product otoacoustic emissions constitute a mixture of emissions. These emissions arise not simply from two distinct cochlear locations but more importantly by two fundamentally different mechanisms: nonlinear distortion induced by the traveling wave and linear, coherent reflection from pre-existing micro-mechanical impedance perturbations of the cochlear partition. Two predictions of the two-mechanism model were tested in their study. The first prediction is that DPOAEs evoked by frequency-scaled stimuli (e.g. at a fixed  $f_2/f_1$  ratio) can be unmixed into distortion-source and reflection-source components with the frequency dependence of their phases consistent with presumed mechanisms of generation. The second prediction is that the reflection-source component of the total DPOAE closely matches the reflection-source emission (e.g., low level stimulus frequency emission)

measured at the same frequency under similar conditions. The DPOAE distortion-source and reflection-source components separated via two completely different separation methods, did, indeed, support the model predictions. Kalluri and Shera (2001) concluded that the fundamental distinction between the two sources is evidently not only source location, but also source mechanism.

In summary, there are two sources that contribute to lower-sideband DPOAEs. The first generation source is the nonlinear interaction between the two primaries close to the  $f_2$  place. The secondary source is the linear reflection at the characteristic site of the particular DP frequency. The clinical interpretation of DPOAE responses is made more difficult by this two-source model. Clinically, DPOAEs are measured at one level with a fixed  $f_2/f_1$  ratio and  $f_2$  at audiometric frequencies, as a correlate of threshold measurement. There are problems with this approach. First, the frequency specificity of DPOAE measurement may be compromised if DPOAE are mixtures of emissions from at least two different regions in the cochlea. Second, the etiological specificity of DPOAE measurement may be compromised if DPOAEs are mixtures of emissions arising from two fundamentally different mechanisms. The recorded DPOAEs should be interpreted as a vector sum of the two sources.

In order to fully understand DPOAEs and interpret clinical results the interaction between the two generation sources must also be investigated. Does the interaction explain the bandpass characteristic of DPOAEs? Does it explain DPOAE fine structure?

#### 1.4. Interactions between two sources

Stover, Neely, and Gorga (1999) stated that the bandpass characteristic of DPOAEs is the result of the interaction between the two generation sources. The DPOAEs recorded from normal hearing subjects showed the bandpass shape. This bandpass shape had two features. First, the peak of the DPOAE frequency function approached  $f_2$  and the bandwidth narrowed as  $f_2$  increased in frequency. Second, there was a shift in peak frequency as stimulus level was reduced. Among hearing impaired subjects, three configurations of hearing loss were investigated. The first had normal hearing at both  $f_2$  and  $f_{dp}$  frequencies with hearing loss in other regions. The second had normal hearing in the  $f_2$  region with hearing loss in the  $f_{dp}$  region. The third had normal hearing in the  $f_{dp}$  region with hearing loss in the  $f_2$  region. The results showed that when the  $f_2$  region and the  $f_{dp}$  region were intact, the patterns of acoustic distortion were essentially normal. When the  $f_2$  region was slightly damaged, the DPOAE was reduced in amplitude but the peak was not systematically shifted from the normal response. When the  $f_{dp}$  region was damaged the response pattern changed to a monotonically decreasing shape, which is similar to that seen in psychophysical measures of distortion. An interaction between the two sources is

one way, maybe the easiest way, to explain the results from this experiment. The response pattern from normal hearing subjects demonstrated this interaction between the two sources. The two sources located near the  $f_2$  and  $f_{dp}$  places did not change cochlear location with changes in level. Therefore, the cancellation of the DPOAE amplitude would remain constant. However, the amount of cancellation might change with level because of the different saturation rates and amplitudes of the two sources. When the  $f_2$  region was slightly damaged, but the  $f_{dp}$  region remained intact the bandpass shape would be the same but the amplitude of DPOAE was reduced, because the interaction of two generation sources would remain as long as the DPOAEs could be generated at the  $f_2$  place. When the  $f_{dp}$  region was damaged, the DPOAE amplitude showed monotonically decreasing shape, because the interaction between two generation sources disappeared. This explained why the normal DPOAE responses have a bandpass shape rather than a monotonically decreasing shape, because of a cancellation interaction between the two generation sources, when  $f_1$  approaches  $f_2$ .

Several different researchers (Gaskill, 1996; Brown, 1996; Heitmann, Waldmann, Schnitzler, 1998; Talmadge, Tubis, Long 1998; and Kalluri et al., 2001) suggested that the lower-sideband DPOAE fine structure found in human subjects is the result of the interference of the two-generation sources at the  $f_2$  and  $f_{dp}$  sites. Mauermann, Uppenkamp, Van Hengel, and Kollmeier (1999b) supported this hypothesis by using hearing-impaired subjects with different hearing loss configurations. As in Stover et al. (1999) two hearing loss configurations were

investigated, which included a sloping high frequency loss only in the  $f_2$  region, and an upward sloping configuration with hearing loss only in the  $f_{dp}$  region. The results from Mauermann, et al., (1999) showed that when the primaries were located in the region of normal or near normal hearing, but DP frequencies were located in a region of impairment, the distortion product  $2f_1-f_2$  was still observable, but the DPOAE fine structure disappeared. When the DP frequencies fell into a region of normal hearing, fine structure was preserved as long as DPOAEs could be recorded. Mauermann, et al., (1999) stated that the initial generation of DPOAE is due to nonlinear distortion at the primary site close to  $f_2$ . This had been exhibited by the findings that normal thresholds in the  $f_2$  region generated nearly normal DPOAE amplitude. Also, they stated that if only the component generated in the primary region contributes to the emission measured in the ear canal, no fine structure could be observed. When there is also a contribution from the re-emission site at  $f_{dp}$ , a quasiperiodic fine structure is observable. According to this hypothesis, peaks in the fine structure are caused by constructive interference of the two generation sites, and the dips are due to destructive interference of the two generation sites. In other words, the dips are due to phase cancellation between two components.

However Mauermann et al., (1999) could not rule out an alternative hypothesis. Namely, the fine structure of lower-sideband DPOAEs is determined by the local impedance properties of the cochlear partition at the  $f_{dp}$  place. When the  $f_{dp}$  place, the hypothesized DPOAE fine structure source, falls in a damaged region, the

fine structure will disappear. When the  $f_2$  place, the primary DPOAE generation source, falls in a damaged region, with a normal  $f_{dp}$  place, the fine structure can be observed as long as the DPOAE can be observed.

Heitmann et al., (1998) argued that the more direct evidence of the interference of two components is obtained by introducing a third tone as a suppressor close in frequency to the  $f_{dp}$  place. The DPOAE fine structure was either decreased or entirely removed when a suppressor tone was introduced at a frequency near  $f_{dp}$ . Like Mauermann et al., (1999) study, Heitmann et al., can not distinguish between the two hypotheses. An alternative hypothesis could also explain this result. The low-level (up to 50 dB SPL) suppressor tone near  $f_{dp}$  only eliminates the emission generated at the  $f_{dp}$  place, which is the hypothesized source of the DPOAE fine structure. According to the alternative hypothesis, when the suppressor cancelled DPOAE from the fine structure source, the DPOAE fine structure would disappear.

More questions are raised from the study conducted by Mauermann et al (1999a). In that study, three experiments were conducted in order to explain the interference of two components of DPOAEs. The first experiment investigated the effect of the frequency ratio  $f_2/f_1$  on the fine structure patterns of the DPOAE at  $2f_1-f_2$ . They predicted that if the local impedance properties of the reflection site near the characteristic  $f_{dp}$  place play a major role in producing DPOAE fine structure, the patterns for different  $f_2/f_1$  ratios would show a high stability when plotted as a function of  $f_{dp}$ . The result showed that the fine structure patterns of  $2f_1-f_2$  shift to

higher frequencies as  $f_2/f_1$  ratio decreases. A pronounced shift occurred when the DPOAE fine structure was plotted as a function of  $f_2$ , and a slight shift was observed when the DPOAE fine structure was plotted as a function of  $f_{dp}$ . The result showed high stability of  $2f_1-f_2$  fine structure patterns. They interpreted this as strong evidence that the local impedance properties of the cochlear partition at the  $f_{dp}$  place played a major role in generating DPOAE fine structure. This is consistent with the  $f_{dp}$  place hypothesis for DPOAE fine structure.

In Mauermann et al., (1999) second experiment, two test conditions were used. In each test condition, three recordings were made. The  $2f_1-f_2$  DPOAE, the  $3f_1-f_2$  DPOAE and the  $4f_1-3f_2$  DPOAE were recorded respectively in each test condition. The frequency ratios were chosen to make constant distance between  $f_2$  and  $2f_1-f_2$ ,  $f_2$  and  $3f_1-2f_2$ ,  $f_2$  and  $4f_1-3f_2$  for each recording respectively in the first test condition. In the second test condition, the frequency ratios were chosen to make constant distance between  $f_1$  and  $2f_1-f_2$ ,  $f_1$  and  $3f_1-2f_2$ ,  $f_1$  and  $4f_1-3f_2$  for each recording respectively. So, when three  $f_2/f_1$  ratios were chosen at 1.22, 1.137, and 1.099, as the frequency swept along the cochlear partition, the identical  $f_2$  frequency could be obtained for all three recording groups. The  $2f_1-f_2$  DPOAE in the first group, the  $3f_1-2f_2$  DPOAE in the second group, and the  $4f_1-3f_2$  DPOAE in the third group would have identical frequency too. The distance between the  $f_2$  place and the  $2f_1-f_2$  DP place in the first group, the  $f_2$  place and the  $3f_1-2f_2$  DP place in the second group and the  $f_2$  place and the  $4f_1-3f_2$  DP place in the third group would be constant and kept the same in three groups. When the three  $f_2/f_1$  ratios were chosen at 1.22, 1.11, and

1.073, as the frequency swept along the cochlear partition, the identical  $f_1$  frequency could be obtained for all three ratio groups. As in the first test condition, the  $2f_1-f_2$  DPOAE, the  $3f_1-2f_2$  DPOAE, and the  $4f_1-3f_2$  DPOAE in the first, the second, and the third group would have identical frequency. However, the distance between the  $f_2$  and  $f_{dp}$  places would not be the same in different groups because the  $f_2$  frequency is not identical in the different groups. As a result, if the DPOAE fine structure is mainly caused by interaction of two components, measurements for DPOAEs (the  $2f_1-f_2$ , the  $3f_1-2f_2$ , and the  $4f_1-3f_2$ ) with identical  $f_2$  and  $f_{dp}$  frequencies should result in very similar patterns, since the interference between the  $f_2$  and  $f_{dp}$  is the same. With identical  $f_1$  and  $f_{dp}$ , no similarity in fine structure should be observed since the interference between two generation sources was varied. The results showed that similar DPOAE fine structure patterns were obtained for both conditions (constant distance between  $f_2$  and  $f_{dp}$ , and varied distance between  $f_2$  and  $f_{dp}$ ). This result supported the hypothesis that local impedance properties of the  $f_{dp}$  place determine the fine structure of DPOAEs rather than the interference of the two generation sources. That is because the similar fine structure patterns could be obtained from either the constant or the varied interference between the  $f_2$  and  $f_{dp}$ , as long as the  $f_{dp}$  place is the same.

In Mauermann et al., (1999) third experiment, the DPOAE fine structure was measured with either fixed  $f_2$  or fixed  $f_{dp}$ . If the fine structure of the DPOAE is dominated by the contribution from the characteristic  $f_{dp}$  place, it is expected that the observable pattern will have less fine structure when  $f_{dp}$  is held constant than when  $f_2$

is fixed. The result showed that the DPOAE fine structure could be observed when  $f_2$  was held constant, and a smooth pattern was obtained when  $f_{dp}$  was held constant. This strongly suggests that the DPOAE fine structure is dominated by the local impedance properties of  $f_{dp}$  place.

Theoretically, if the DPOAE fine structure were contributed only by the interference of two generation sources, the fine structure of stimulus frequency otoacoustic emission would not be expected because it has only one otoacoustic emission source. In fact, the fine structure of SFOAE can be found in human subjects (Harris & Brown 1994, Stover & Norton 1993). The hypothesis that the DPOAE fine structure is the result of the interference between two cochlear origination sources (the  $f_2$  and  $f_{dp}$  sites) does not seem to be supported by data. An alternative hypothesis that irregularity in the impedance property of the cochlear partition at the characteristic  $f_{dp}$  place is the main cause of the fine structure of the lower-sideband DPOAEs is supported by the data. The impedance property of the cochlear partition at the characteristic  $f_{dp}$  place appears to be the primary source of the DPOAE fine structure since the late component of lower-sideband DPOAEs is generated from a fixed position of the cochlear partition at the  $f_{dp}$  site. The interference of the two generation sites will cancel each other when the two primaries get closer and lead to the bandpass characteristic of the DPOAE (Stover et al. 1999).

The goal of the proposed research is to investigate whether the DPOAE fine structure is caused by the interference of two DPOAE generation sources or is mainly caused by the impedance property of the cochlear partition itself at the  $f_{dp}$  generation site. The specific hypothesis in this study is that the  $2f_1-f_2$  DPOAE fine structure is dominated by the local impedance property of the cochlear partition at the characteristic DP place. This experiment has been designed to measure the DPOAE fine structure under different stimulus configurations based on the assumption that the late component of the  $2f_1-f_2$  DPOAE is always generated from a fixed position on the cochlear partition at the  $f_{dp}$  place. Five different stimulus protocols were designed to find out whether the local impedance property of the cochlear partition at the characteristic DP place mainly contributes to the fine structure of DPOAE. This experiment focused on  $2f_1-f_2$  DPOAEs.

The clinical potential of this line of research is to improve early diagnostic tests of hearing loss in infants and neonates. The previous studies (Mauermann et al., 1999; Talmadge, Tubis, Long, and Tong, 2000; Kalluri and Shera, 2001) have indicated that the  $2f_1-f_2$  DPOAE fine structure appears to be a more sensitive indicator of cochlear damage than DPOAE alone.

## **CHAPTER 2**

### **METHODOLOGY**

#### 2.1. Subjects

Two male and three female, normal-hearing subjects, ranging in age from 22 to 41 years (average 27.6 years), participated in this experiment. All subjects' hearing thresholds were better than 20 dB HL for all audiometric frequencies in the range 250 Hz to 8000 Hz. All subjects had normal middle ear immittance and a negative history of otological disease or prolonged exposure to high levels of noise. For each subject 358 DPOAEs were recorded using five different test protocols (Table 1). In order to demonstrate data reliability, all five protocols were measured twice. Each subject was asked to sit in a comfortable recliner in a sound treated booth and remain as quiet as possible for one- to three hours for each session. Approximately five- to seven hours were used for each subject.

#### 2.2. Signals

Signals were generated digitally by Tucker-Davis Technology (TDT) SigGen software and played via TDT D/A converters. Sinusoids were passed through programmable attenuators (TDT PA4), and presented through insert earphones

(Etymotic ER10C) in an ear-canal microphone assembly. Ear canal sound pressure was measured by the microphone of the ER10C and digitized via a TDT A/D converter. A PC computer controlled signal and experimental parameters using the TDT software, BioSig. The DPOAE responses were averaged over 100 stimulus presentations and were stored as a time waveform.

### 3.3. Testing protocols

Five protocols were designed to test the  $f_{dp}$  place hypothesis. These five protocols covered four degrees of freedom in the stimulus space by fixing the  $f_2/f_1$  ratio,  $f_2$ ,  $f_1$ , or  $f_{dp}$ . Each protocol was designed to hold one aspect of DPOAE generation constant, based on the following assumptions. 1) The DPOAE is generated at two different cochlear locations specifically associated with the  $f_2$  and  $f_{dp}$  places. 2) The primary generator site is slightly apical to the  $f_2$  place and is “wave-fixed”. 3) The secondary generator site is at the  $f_{dp}$  place and is “place-fixed”. These assumptions are supported by the previous studies (Kalluri and Shera, 2001; Mauermann et al., 1999).

Protocol 1 used a fixed  $f_2/f_1$  ratio. According to the  $f_{dp}$  place hypothesis, under this condition: a) the interference between the two DPOAE generation sources is constant because the distance between the  $f_2$  and  $f_{dp}$  places is constant on a logarithm scale. The two primaries move along the cochlear partition together with a constant  $f_2/f_1$  ratio. b) the  $2f_1-f_2$  DPOAE late component fine structure is due to the cochlear

irregularities at the  $f_{dp}$  place. c) the  $2f_1-f_2$  DPOAE early component will not have fine structure. The ratio  $f_2/f_1$  was kept at 1.2, since this ratio generates the largest  $2f_1-f_2$  amplitude (Stover, Gorga, Neely 1996).

Protocol 2  $f_2$  fixed at 4000 Hz and swept  $f_1$ . The  $f_2/f_1$  ratio varied as frequency changed. According to the  $f_{dp}$  place hypothesis, under this condition: a) the interference between two DPOAE generation-sources is variable. Only the lower frequency primary ( $f_1$ ) moves along the cochlear partition; as it increases in frequency,  $f_1$  approaches the higher frequency primary ( $f_2$ ); b) the  $2f_1-f_2$  DPOAE late component fine structure is due to the cochlear irregularities at the  $f_{dp}$  place. c) the early component of the  $2f_1-f_2$  DPOAE would fix near the  $f_2$  place and no fine structure would be observed. In order to compare the DPOAE fine structure at the  $f_{dp}$  place, protocol 1 and 2 used the same  $f_{dp}$  frequency range (1600 Hz to 3200Hz).

Protocols 3 & 4  $f_1$  fixed at 3000 Hz and 2800 Hz, respectively, and swept  $f_2$ . The  $f_2/f_1$  ratio varied with frequency. According to the  $f_{dp}$  place hypothesis, under this condition: a) the interference between the two DPOAE generation sources is variable. The higher frequency primary ( $f_2$ ) moves along the cochlear partition. As frequency sweeps, the two generation sources (at the  $f_2$  and  $f_{dp}$  places) move away from the lower frequency primary ( $f_1$ ) in opposite directions. b) The fine structure of the  $2f_1-f_2$  DPOAE late component is due to the cochlear irregularities at  $f_{dp}$  place. c) The early component will not have fine structure. In order to make comparisons of the DPOAE fine structure at the  $f_2$  and  $f_{dp}$  places with data from protocol 1, two  $f_1$

regions were chosen. When  $f_1$  equaled 3000 Hz, the  $f_{dp}$  frequency range (1600 Hz to 2960 Hz) was in the same range as in protocol 1. When  $f_1$  equaled 2800 Hz, the  $f_2$  frequency range (2850 Hz to 4200 Hz) was the same as in protocol 1.

Protocol	$f_2$	$f_1$	$f_{dp}$	$f_2/f_1$ ratio	Number of records
1	2400-4800Hz 30Hz steps	2000-4000Hz 25Hz steps	1600-3200Hz 20Hz steps	Fixed at 1.2	81
2	Fixed at 4000Hz	2800-3600Hz 10Hz steps	1600-3200Hz 20Hz steps	1.11-1.43	81
3	3040-4400Hz 20Hz steps	Fixed at 3000Hz	1600-2960Hz 20Hz steps	1.01-1.47	69
4	2850-4200Hz 30Hz steps	Fixed at 2800Hz	1400-2750Hz 30 Hz steps	1.02-1.5	46
5	2400-4800Hz 30Hz steps	2360-3560Hz 15Hz steps	Fixed 2320Hz	1.02-1.35	81

**Table 1. Summary of five DPOAE data collection protocols for this study.**

Protocol 5 the  $f_{dp}$  fixed at 2320 Hz, and swept both  $f_1$  and  $f_2$ . The  $f_2/f_1$  ratio varied. According to the  $f_{dp}$  place hypothesis, under this condition, a) the interference between the two DPOAE generation sources is variable because the distance between the  $f_2$  and  $f_{dp}$  places is changing. The two primaries move along the cochlear partition at different speeds. The  $f_2$  tone moves faster than the  $f_1$  component. b) the fine structure of fine structure of the  $2f_1-f_2$  DPOAE late

component is minimal because the late component generation place  $f_{dp}$  is fixed. c) the  $2f_1-f_2$  DPOAE early component will not have fine structure. In order to make a comparison of the amplitude of DPOAE responses at the  $f_2$  place, the  $f_2$  frequency range (2400 Hz to 4800 Hz) was the same as in protocol 1.

The primary intensity,  $L_1$  was set to 65 dB SPL and  $L_2$  equaled 55 dB SPL for all five protocols, since these intensity levels tend to produce the most robust  $2f_1-f_2$  distortion product (Stover et al., 1996).

#### 2.4. Data collection

The frequency, amplitude, and phase of the DPOAEs were recorded for further analysis. For each condition, the data were measured by using the BioSig software and stored as a time waveform shown as Figure 2a.

#### 2.5. Data analysis

The frequency, amplitude, and phase of both primary tones, and each of three distortion products ( $2f_1-f_2$ ,  $3f_1-2f_2$ , and  $2f_2-f_1$ ), and an estimate of the noise floor were measured from the power spectrum of the waveform using Matlab's FFT (Fig. 2b). The Matlab program is given in Appendix 1. Then, the amplitude of the  $2f_1-f_2$  DPOAEs was obtained across the swept frequencies for each of the protocols (Fig. 2c). Each point in figure 2c corresponds to one DPOAE time wave. This frequency domain representation of the DPOAE was then transformed to the time domain (for

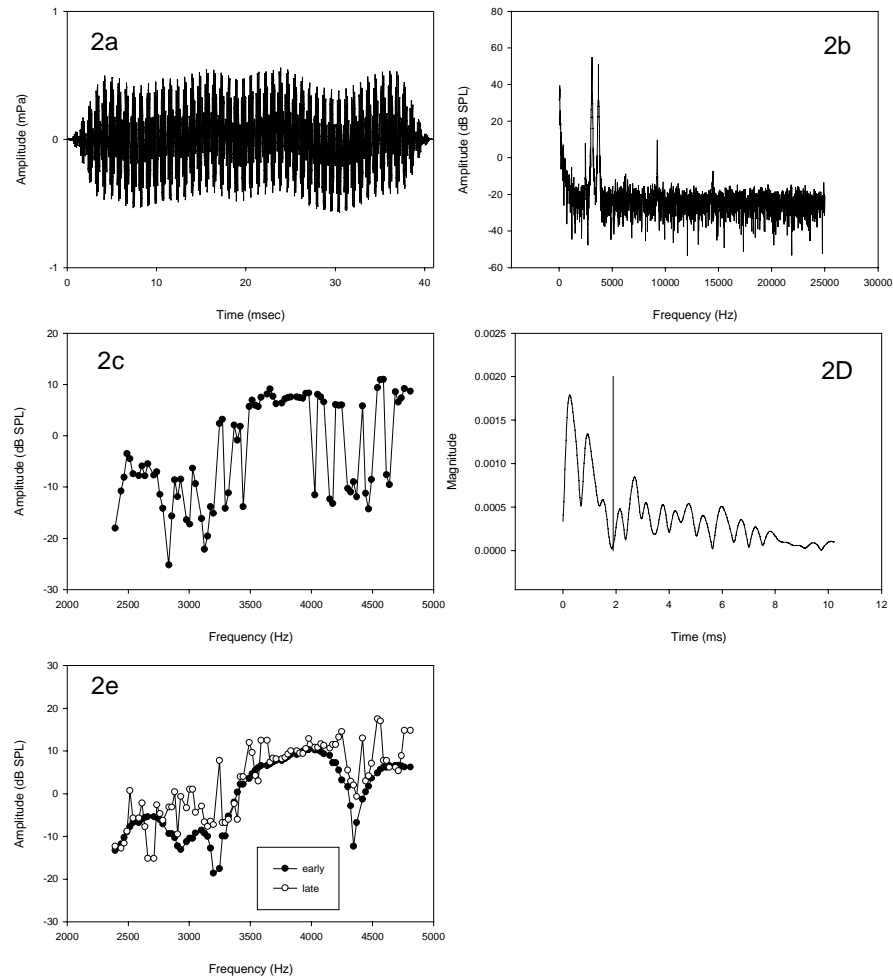


**Figure 2: Illustration of the various steps of data processing. (a) DPOAE time waveform. (b) DPOAE power spectrum. (c) The amplitude of  $2f_1-f_2$  DPOAE across swept frequencies. (d) Figure 2c has been transformed to the time domain using an inverse FFT. The vertical line indicates the time window that separates the DPOAE early and late components. (e) Each component has been transformed back to frequency domain via a FFT. The solid dot represents the early component and the circle represents the late component.**

each of the protocols) using an inverse FFT (Fig. 2d). This time domain representation, akin to an impulse response, showed several peaks, indicating multiple latency.

According to the two-source hypothesis, the higher amplitude latency peaks are contributed by the early component of DPOAEs, and the rest of the peaks are contributed by the late component of DPOAEs. In the final step, the data were windowed in the latency domain into early and late components before each component was transformed back to the frequency domain using a FFT (Fig. 2e).

A comparison of the complete  $2f_1-f_2$  DPOAE amplitude versus its late component amplitude was made for each of the protocols for each subject. If the complete  $2f_1-f_2$  DPOAE and its late component have similar fine structure patterns in terms of similar peak-to-peak frequency space and peak-to-valley level differences, the  $f_{dp}$  place hypothesis will be supported.

Four comparisons of the separated DPOAE early component amplitudes or DPOAE late component fine structure were made. First, the  $2f_1-f_2$  DPOAE early components were compared for the fixed  $f_2/f_1$  ratio and the  $f_1$  fixed at 2800 Hz protocols. Second, the amplitude of the  $2f_1-f_2$  DPOAE early components were compared between the fixed  $f_2/f_1$  ratio protocol and fixed  $f_{dp}$  protocol. According to the  $f_{dp}$  place hypothesis, no fine structure would be expected from these early components. Also, for the same  $f_2$  frequency range (2400 Hz to 4800 Hz), these early components obtained from different protocols would not be expected to have

the same amplitude because the  $f_2/f_1$  ratio was fixed or varied. Third, the  $2f_1-f_2$  DPOAE late components were compared for the fixed  $f_2/f_1$  ratio protocol and fixed  $f_2$  protocol. Finally, the  $2f_1-f_2$  DPOAE late components were compared for the fixed  $f_2/f_1$  ratio protocol and  $f_1$  fixed at 3000 Hz protocol. According to the  $f_{dp}$  place hypothesis, these late components are the cochlear response at the  $f_{dp}$  place for the same  $f_{dp}$  range (1600 Hz to 3200 Hz). All comparisons were plotted either as a function of  $f_2$  (early component comparisons) or  $f_{dp}$  (late component comparisons) using SigmaPlot software.

A fine structure index was calculated to indicate the degree of fine structure. Two numbers defined the fine structure index. The first number is the average frequency difference between adjacent peaks in the fine structure across each test protocol as shown in Figure 3, measurement “A”. The frequency difference is indicated in octave. The second number is the average of peak-to-valley level difference in the fine structure across each of the protocols as shown in Figure 3, measurement “B”. The smaller frequency space between the adjacent peaks and greater peak-to-valley level difference indicate the high degree of fine structure. The fine structure indices were calculated by hand based on the measurement of the amplitude of the whole  $2f_1-f_2$  DPOAEs and the amplitude of the separated early and late components.

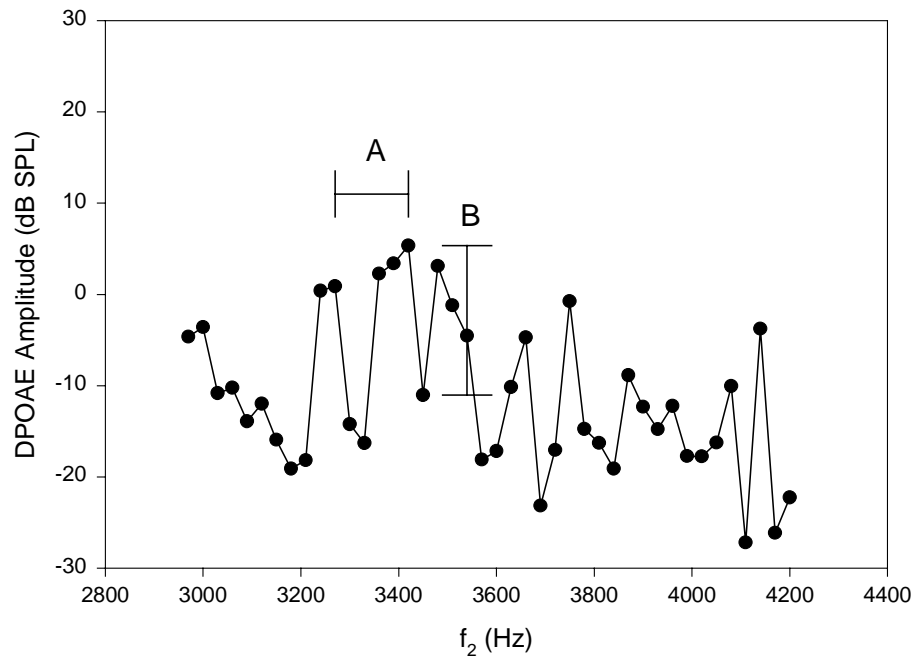


**Figure 3: Illustration of the measurement of the fine structure index. A represents the peak-to-peak frequency space. B represents the peak-to-valley level difference.**

The phase of the complete DPOAE and two components (early vs. late) were always referred to the primary stimuli,  $f_1$  tone. All phases were unwrapped using a Matlab program that provided in Appendix 3.

All comparisons, which include comparisons of DPOAE fine structure and comparisons of phase made in this experiment, were within-subject and across-protocol comparisons, or within-subject and within-protocol comparisons. Previous work (He and Schmiedt, 1993) stated that fine structure patterns differ from subject to subject. Thus, no comparison was made across the subjects.

## CHAPTER 3

### RESULTS

#### 3.1. Data replication

The DPOAEs were measured twice under each of the protocols in order to reduce the influence of random fluctuation and to demonstrate reliability. The two DPOAE measurements were conducted on two different days within one week for each subject. Figure 4 shows the  $2f_1-f_2$  DPOAE amplitude recorded twice using the fixed  $f_2/f_1$  ratio protocol for all five subjects. Visual inspection of the repeated measurements indicated consistent fine structure and reliable replication.

#### 3.2. Fine structure

The  $2f_1-f_2$  DPOAEs recorded from all five subjects show obvious fine structure for each of the first four protocols (Fig., 5, 6, 7, and 8). The  $2f_1-f_2$  DPOAE amplitude was plotted as a function of  $f_2$  on a linear scale for the fixed  $f_2/f_1$  ratio and  $f_1$  fixed at 2800 Hz protocols. For the fixed  $f_2$  and  $f_1$  fixed at 3000 Hz protocols, the  $2f_1-f_2$  DPOAE amplitude was plotted as a function of  $f_{dp}$  on a linear scale. For the fixed  $f_2/f_1$  ratio protocol, the fine structure appears to be relatively smoother in the  $f_2$  frequency range of 3500 Hz to 4000 Hz for all five subjects. For the  $f_1$  fixed at 3000

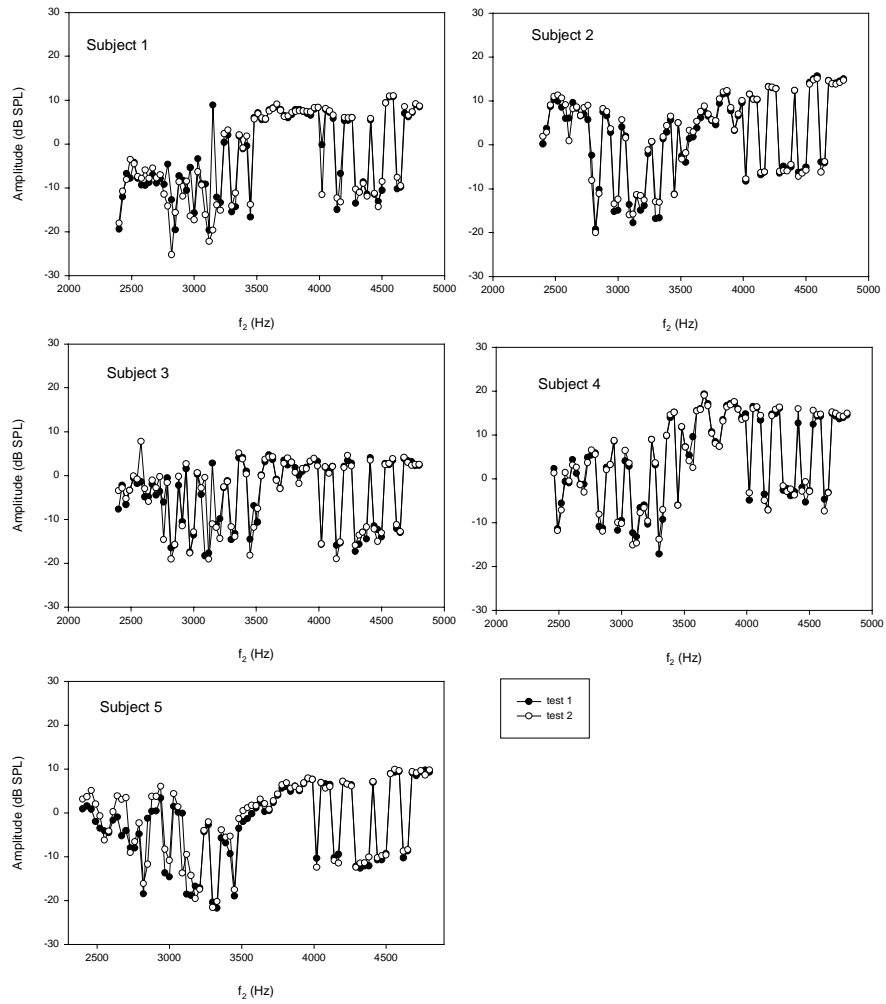


**Figure 4: Illustration of replicability of the DPOAEs. Amplitude of the  $2f_1 - f_2$  DPOAE of two measurements using the fixed  $f_2/f_1$  ratio protocol is plotted as a function of  $f_2$ . Data for each subject are shown in a separate panel.**

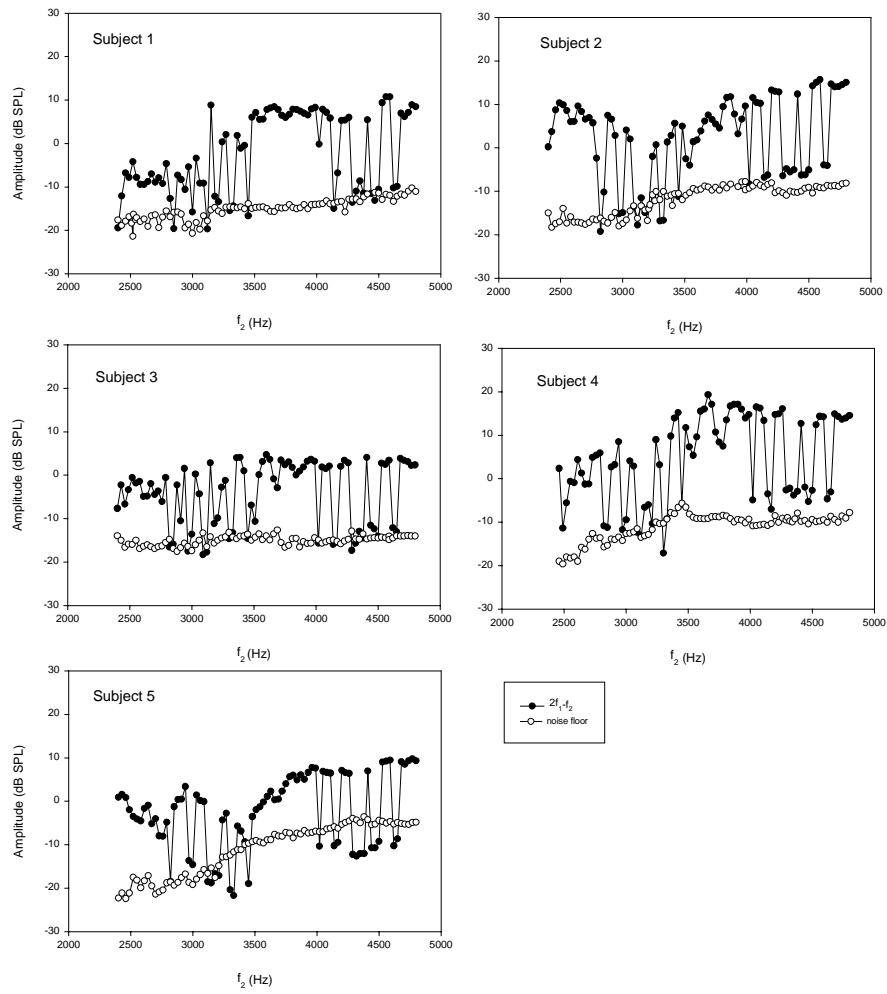


**Figure 5: The amplitude of the  $2f_1-f_2$  DPOAE using the fixed  $f_2/f_1$  ratio protocol is plotted as a function of  $f_2$  for the first measurement. The estimated noise floor is averaged across the five protocols for each subject. The solid dot represents the amplitude of the  $2f_1-f_2$  DPOAE. The circle represents the estimated noise floor. Data for each subject are shown in separate panel.**

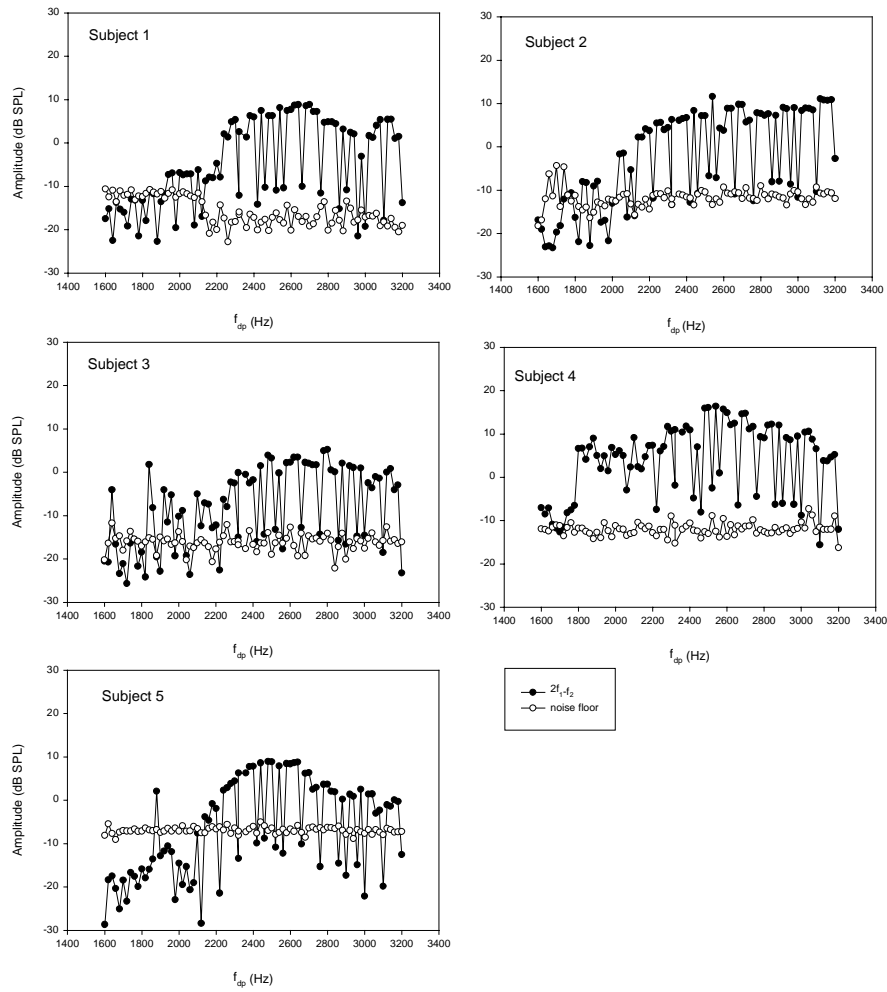


**Figure 6: The amplitude of the  $2f_1-f_2$  DPOAE using the  $f_2$  fixed at 4000Hz protocol is plotted as a function of  $f_{dp}$  for the first measurement. The estimated noise floor is averaged across the five protocols for each subject. The solid dot represents the amplitude of the  $2f_1-f_2$  DPOAE. The circle represents the estimated noise floor. Data for each subject are shown in separate panel.**

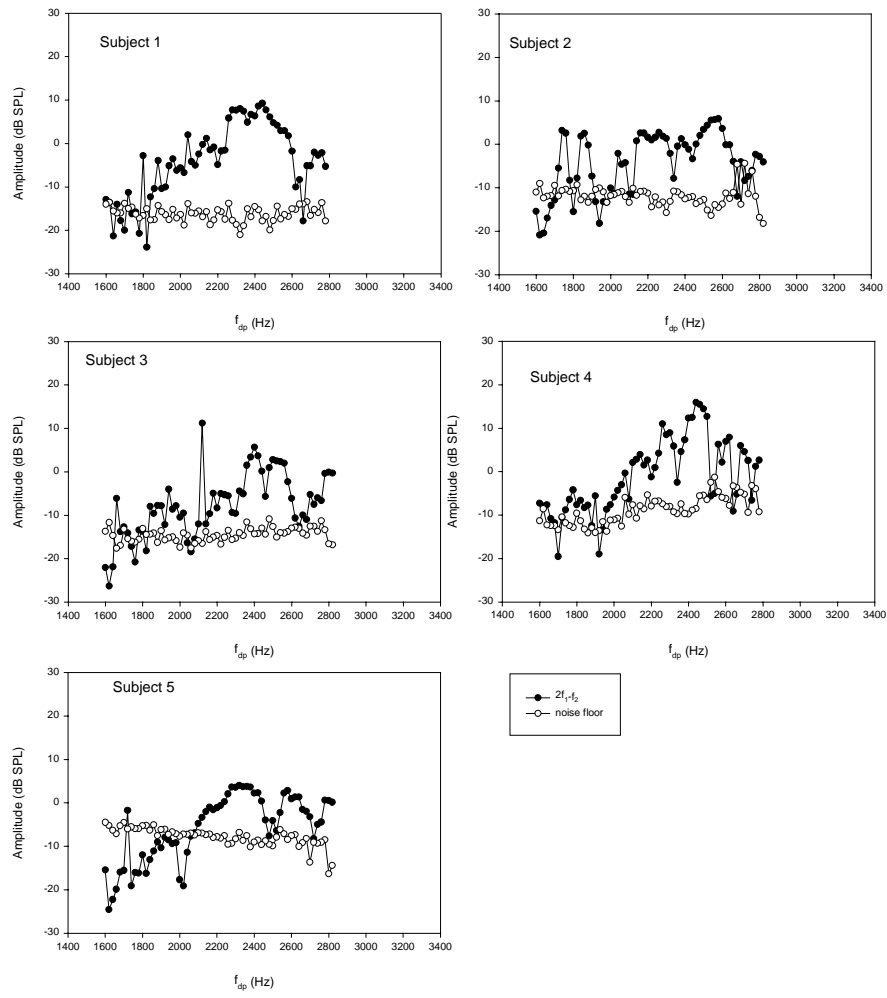


**Figure 7: The amplitude of the  $2f_1-f_2$  DPOAE using the  $f_1$  fixed at 3000 Hz protocol is plotted as a function of  $f_{dp}$  for the first measurement. The estimated noise floor is averaged across the five protocols for each subject. The solid dot represents the amplitude of the  $2f_1-f_2$  DPOAE. The circle represents the estimated noise floor. Data for each subject are shown in separate panel.**

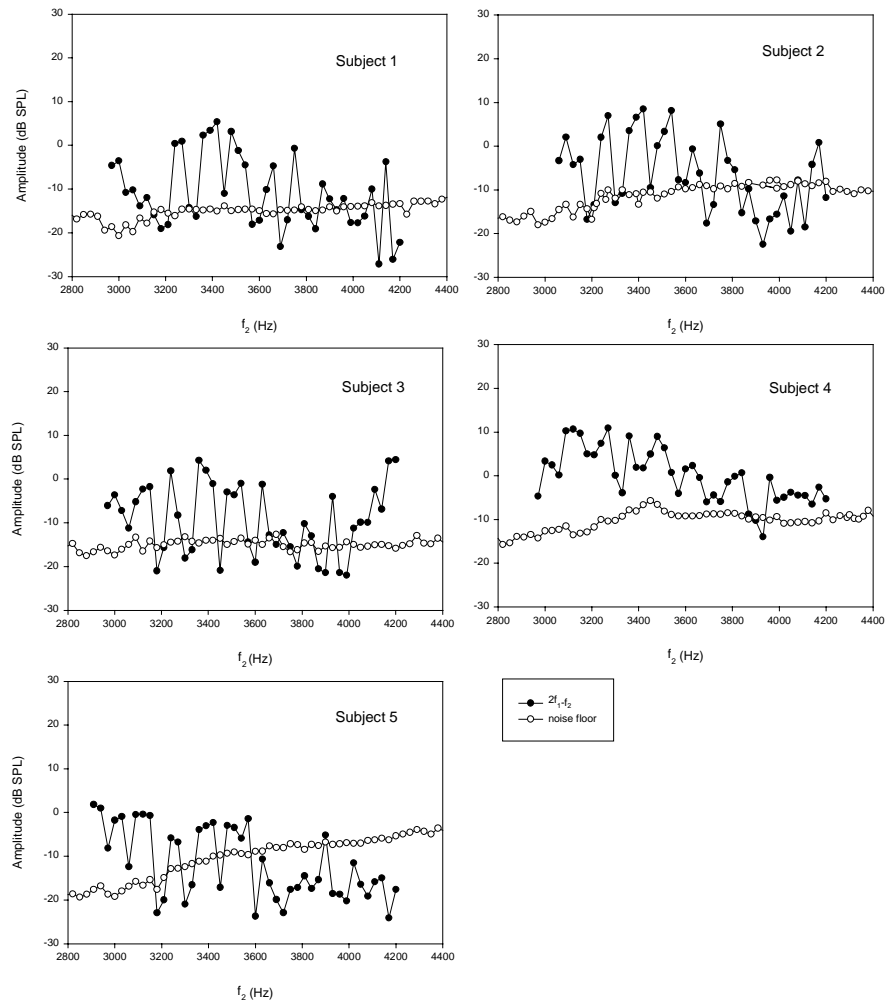


**Figure 8: The amplitude of the  $2f_1-f_2$  DPOAE using the  $f_1$  fixed at 2800 Hz protocol is plotted as a function of  $f_2$  for the first measurement. The estimated noise floor is averaged across the five protocols for each subject. The solid dot represents the amplitude of the  $2f_1-f_2$  DPOAE. The circle represents the estimated noise floor. Data for each subject are shown in separate panel.**

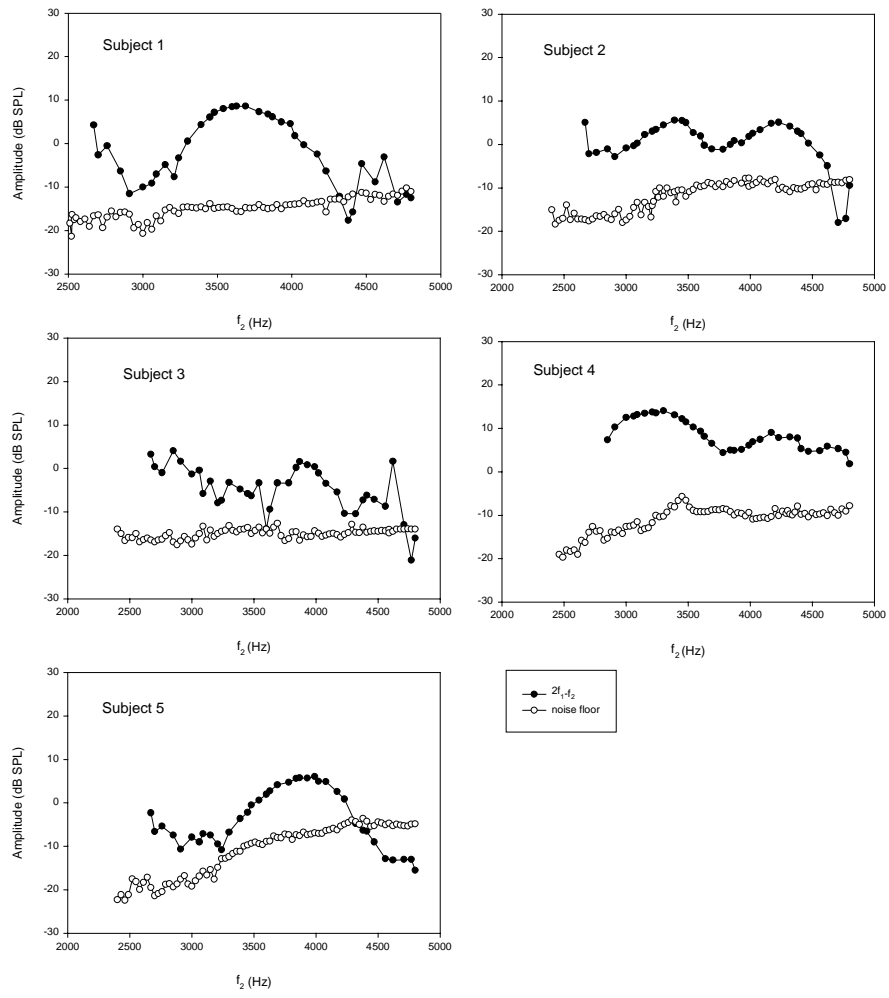


**Figure 9:** The amplitude of the  $2f_1-f_2$  DPOAE using the fixed  $f_{dp}$  protocol is plotted as a function of  $f_2$  for the first measurement. The estimated noise floor is averaged across the five protocols for each subject. The solid dot represents the amplitude of the  $2f_1-f_2$  DPOAE. The circle represents the estimated noise floor. Data for each subject are shown in separate panel.

Hz protocol the fine structure appears to be relatively smoother in the  $f_{dp}$  frequency range of 2000 Hz to 2800 Hz for subject 1, 2, and 5. For the fixed  $f_2$  and  $f_1$  fixed at 2800 Hz protocol, the fine structure with smaller peak-to-peak frequency space and greater peak-to-valley level difference are consistently across the tested frequencies for all five subjects. For subject 5, the  $2f_1-f_2$  DPOAE amplitude was relatively lower and the estimated noise floor was relatively higher than for the other subjects. The fine structure in these figures (Fig. 5, 6, 7 and 8) is consistent with the  $f_{dp}$  place hypothesis. The fine structure pattern is different from subject to subject. Finally, as the  $f_{dp}$  place hypothesis predicted, the  $2f_1-f_2$  DPOAEs showed a smooth bandpass pattern for fixed  $f_{dp}$ , when the amplitude of  $2f_1-f_2$  was plotted as a function of  $f_2$  on a linear scale (Fig.9) for all five subjects.

The fine structure indices for the  $2f_1-f_2$  DPOAE range from 0.044 to 0.09 octave and from 9.12 to 17.85 dB across first four protocols for all five subjects. The peak-to-peak frequency space was less than 0.094 octave and the peak-to-valley level difference was as large as 30 dB and no less than 3 dB as defined in a previous study (He & Schmiedt 1993). The indices indicated that for  $f_1$  fixed either at 2800 Hz or 3000 Hz protocols the DPOAE fine structure tended to have a wider frequency range and smaller peak-to-valley level difference than either the fixed  $f_2/f_1$  ratio and the protocols fixed  $f_2$  did for all five subjects.

	fixed $f_2/f_1$ ratio		Fixed $f_2$ at 4000 Hz		Fixed $f_1$ at 3000 Hz		fixed $f_1$ at 2800 Hz	
	Octave	dB	Octave	dB	Octave	dB	Octave	dB
Subject 1	0.067	15.31	0.044	15	0.07	9.12	0.074	13.28
Subject 2	0.068	15.88	0.05	16.98	0.091	11.77	0.09	15.27
Subject 3	0.053	14.21	0.044	15.95	0.075	10.45	0.086	14.98
Subject 4	0.061	17.85	0.051	14.25	0.068	11.99	0.09	10.67
Subject 5	0.071	15.17	0.047	16.56	0.086	9.65	0.08	11.93

**Table 2: The complete  $2f_1-f_1$  DPOAE fine structures index for the first four protocols, for each of the five subjects.**

### 3.3. Early and late components of $2f_1-f_2$ DPOAE

In order to investigate the source of fine structure, the separated early and late components of the  $2f_1-f_2$  DPOAE are shown as Figure 10, 11, 12, 13 and 14 for each protocol. The amplitude of the early and late components was plotted as a function of  $f_2$  for the fixed  $f_2/f_1$  ratio, the  $f_1$  fixed at 2800 Hz and the fixed  $f_{dp}$  protocols. For the fixed  $f_2$  and the  $f_1$  fixed at 3000 Hz protocols, the amplitude of the early and late components was plotted as a function of  $f_{dp}$ . The separated components from the first four protocols fell into the same pattern from all five subjects (Figure 10, 11, 12 and 13). The early components were smoother with no measurable fine structure. The late components consistently showed high degree fine structure. The separated components for fixed  $f_{dp}$  protocol showed a smooth pattern with no fine structure for either early and late components for all five subjects (Figure 14). This is, again, consistent with the predictions of the  $f_{dp}$  place hypothesis.

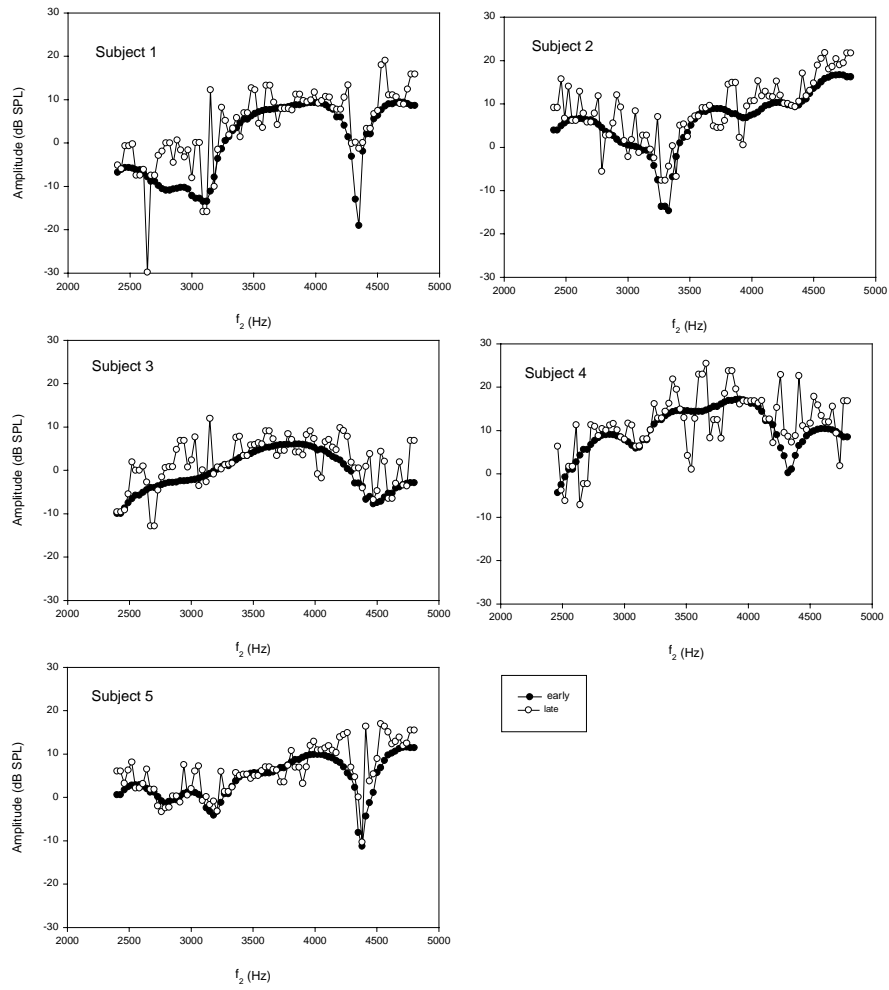


**Figure 10: Amplitude of the separated early and late components using the fixed  $f_2/f_1$  ratio protocol is plotted as a function of  $f_2$  for the first measurement. The solid dot represents the early component. The circle represents the late component. Data for each subject are shown in separate panel.**

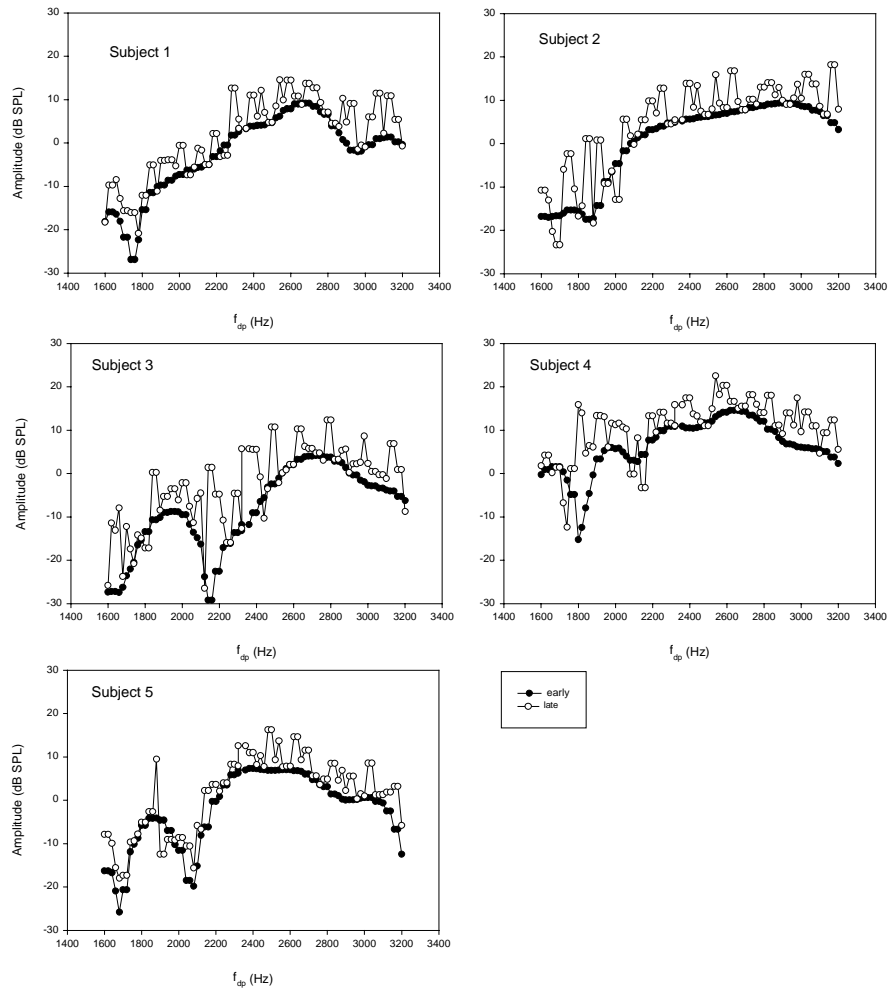


**Figure 11: Amplitude of the separated early and late components using the  $f_2$  fixed at 4000 Hz protocol is plotted as a function of  $f_{ap}$  for the first measurement. The solid dot represents the early components. The circle represents the late component. Data for each subject are shown in separate panel.**

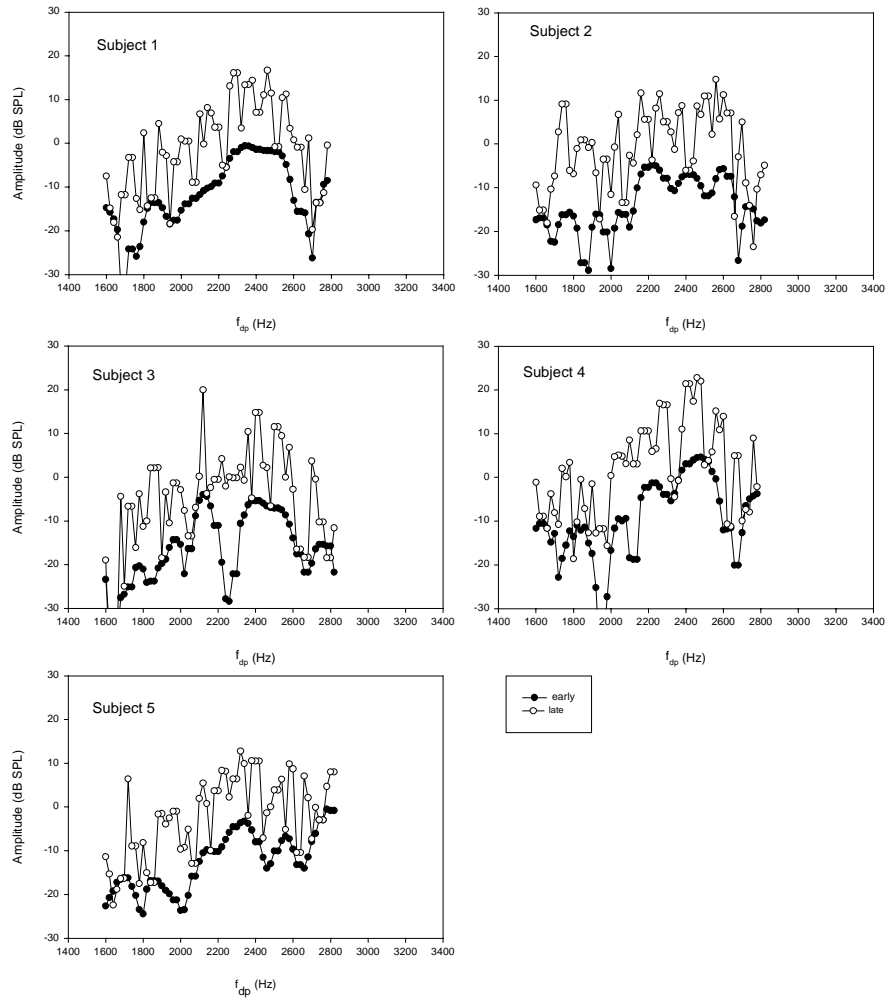


**Figure 12: Amplitude of the separated early and late components using the  $f_1$  fixed at 3000 Hz protocol is plotted as a function of  $f_{dp}$  for the first measurement. The solid dot represents the early component. The circle represents the late component. Data for each subject are shown in separate panel.**

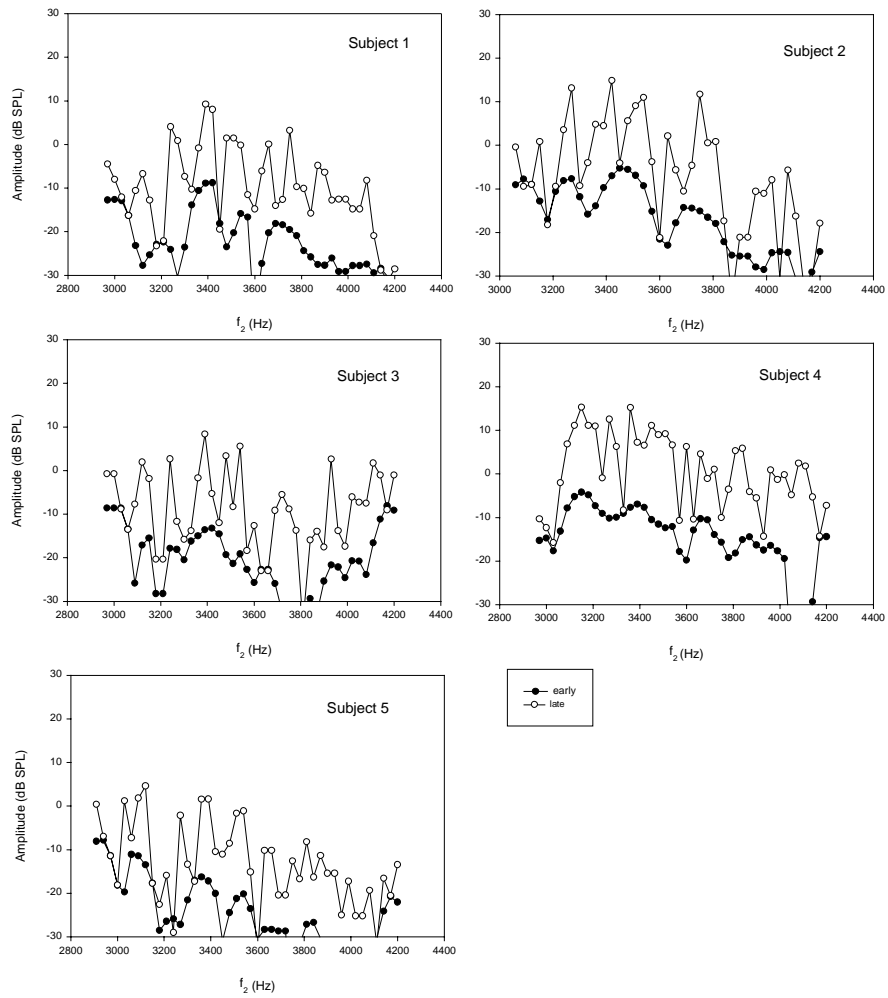


**Figure 13: Amplitude of the separated early and late components using the  $f_1$  fixed at 2800 Hz protocol is plotted as a function of  $f_2$  for the first measurement. The solid dot represents the early component. The circle represents the late component. Data for each subject are shown in separate panel.**

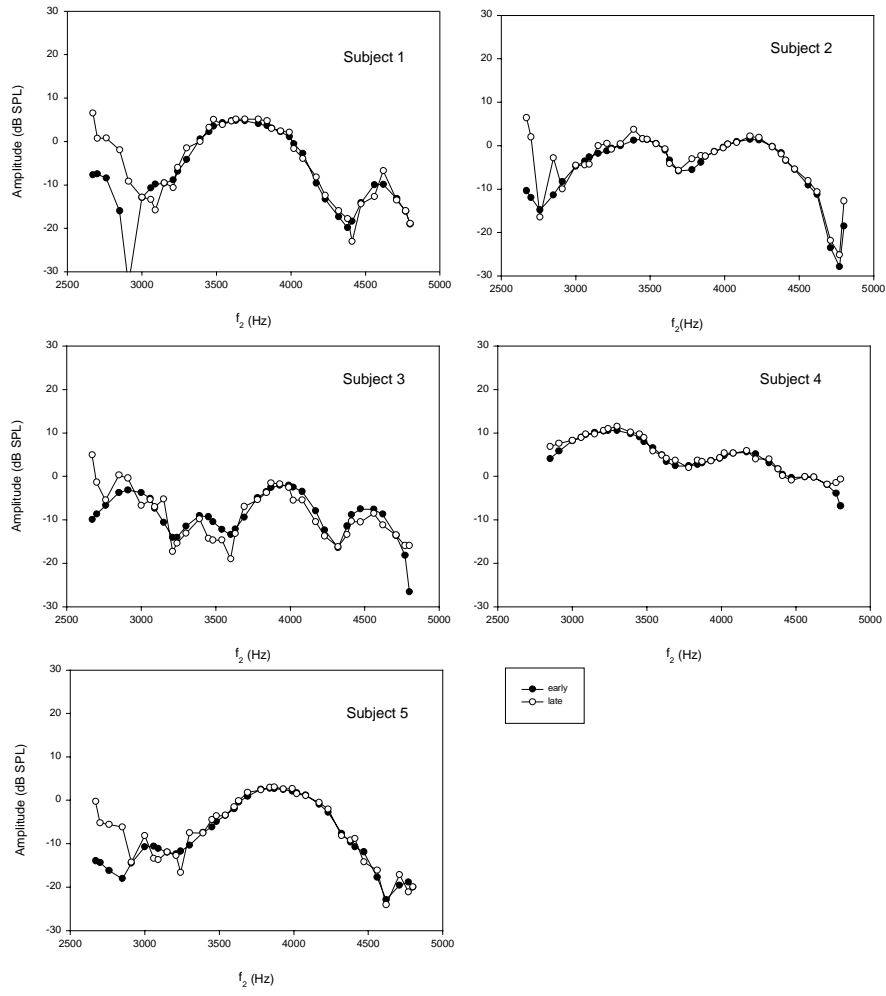


**Figure 14: Amplitude of the separated early and late components using the fixed  $f_{dp}$  protocol is plotted as a function of  $f_2$  for the first measurement. The solid dot represents the early component. The circle represents the late component. Data for each subject are shown in separate panel.**

The  $2f_1-f_1$  DPOAE late component fine structure indices ranged from 0.051 to 0.092 octave and from 8.8 to 21.52 dB for the first four protocols, for each of the five subjects. These fine structure indices showed that the complete  $2f_1-f_1$  DPOAE and its late component have a similar fine structure index.

	fixed $f_2/f_2$ ratio		Fixed $f_2$ at 4000 Hz		Fixed $f_1$ at 3000 Hz		Fixed $f_1$ at 2800 Hz	
	Octave	dB	Octave	dB	Octave	dB	Octave	dB
Subject 1	0.077	10.45	0.056	10.38	0.063	13.56	0.092	16.95
Subject 2	0.059	9.19	0.063	9.36	0.067	14.57	0.091	18.84
Subject 3	0.071	9.79	0.063	11.47	0.051	15.16	0.085	21.52
Subject 4	0.068	12.25	0.068	8.8	0.071	14.8	0.077	17.68
Subject 5	0.092	9.24	0.071	8.83	0.065	13.03	0.067	14.92

**Table 3: Fine structure index of the late component of the  $2f_1-f_1$  DPOAE for the first four protocols, for each of the five subjects.**

#### 3.4. Comparisons

The comparisons between the complete  $2f_1-f_2$  DPOAE and its late component show a similar fine structure pattern in terms of peak-to-peak frequency space and peak-to-valley level differences for the first four protocols, and from all five subjects (Figure 15, 16, 17 and 18). For the fixed  $f_{dp}$  protocol, the complete  $2f_1-f_2$  DPOAE and its late component amplitude have an almost identical smooth pattern for all five subjects (Figure 19).

To reinforce the  $f_{dp}$  place hypothesis four comparisons are shown as Figures 20, 21, 22 and 23. Figure 20 compares the early component amplitude as a function of  $f_2$  for the fixed  $f_2/f_1$  ratio protocol and the  $f_1$  fixed at 2800 Hz protocol for all five

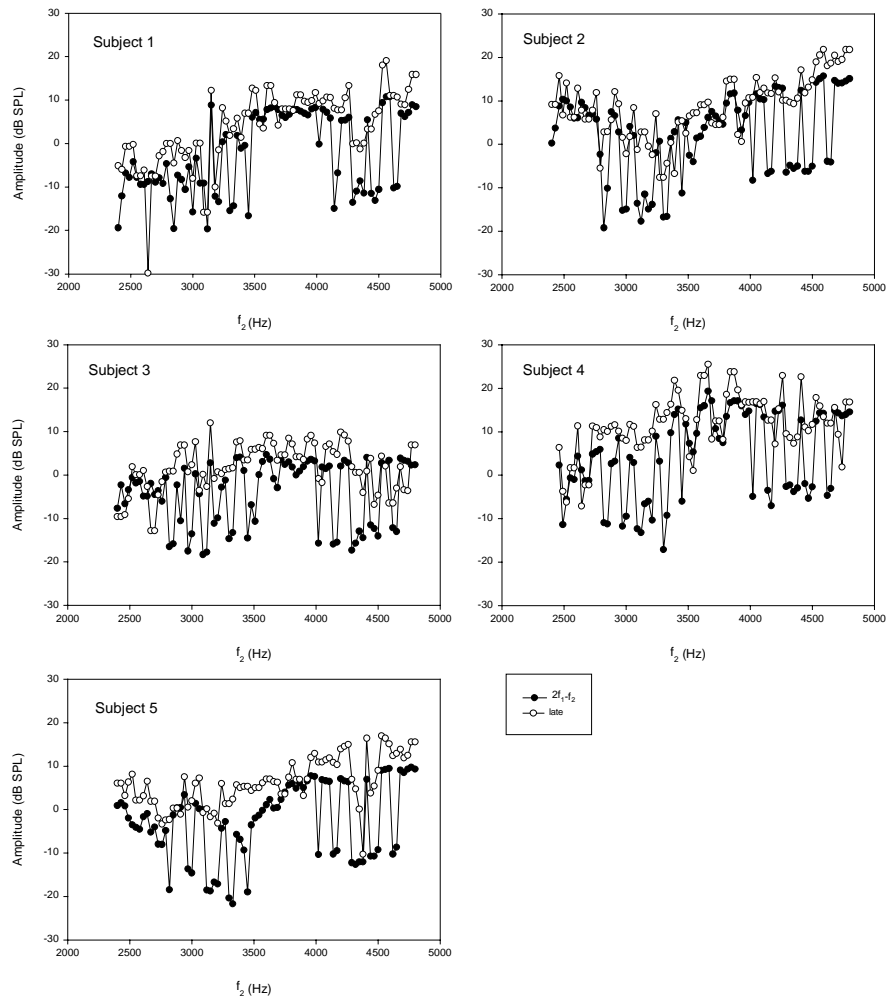


**Figure 15: Amplitude of the complete  $2f_1-f_2$  DPOAE and its late component using the fixed  $f_2/f_1$  ratio protocol is plotted as a function of  $f_2$  for the first measurement. The solid dot represents the complete  $2f_1-f_2$  DPOAE. The circle represents the late component. Data for each subject are shown in separate panel.**

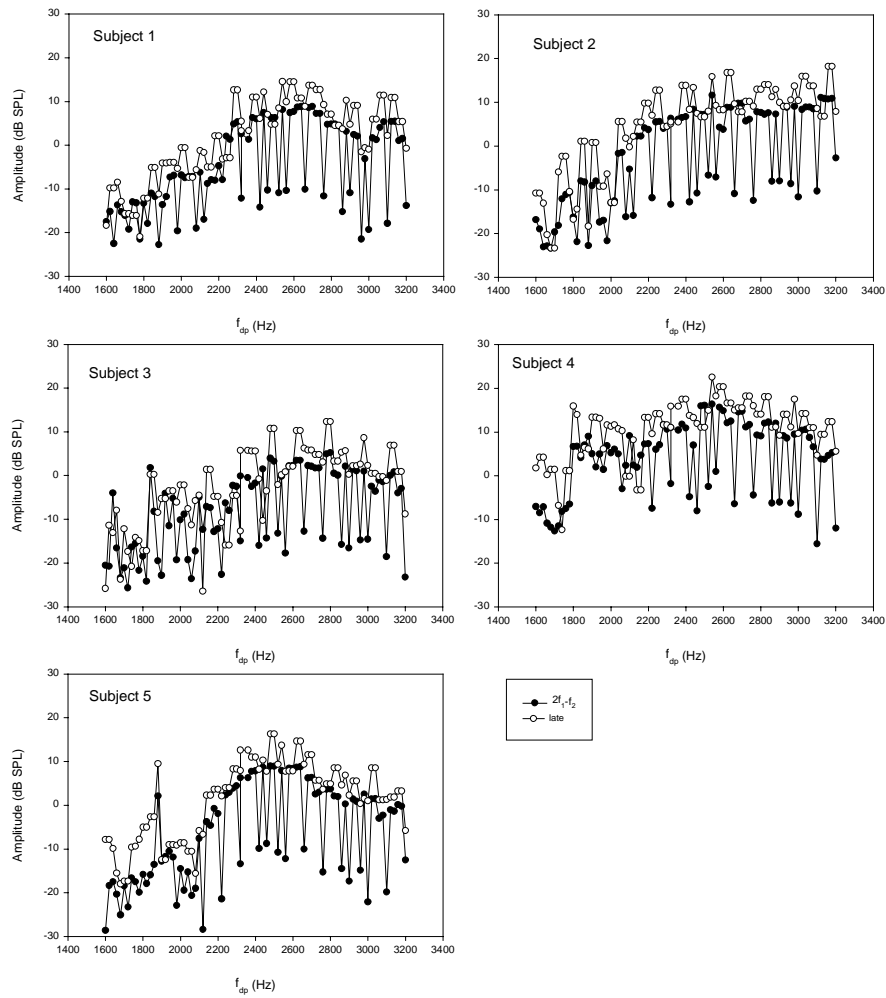


**Figure 16: Amplitude of the complete  $2f_1-f_2$  DPOAE and its late component using the  $f_2$  fixed at 4000Hz protocol is plotted as a function of  $f_{dp}$  for the first measurement. The solid dot represents the complete  $2f_1-f_2$  DPOAE. The circle represents the late component. Data for each subject are shown in separate panel.**

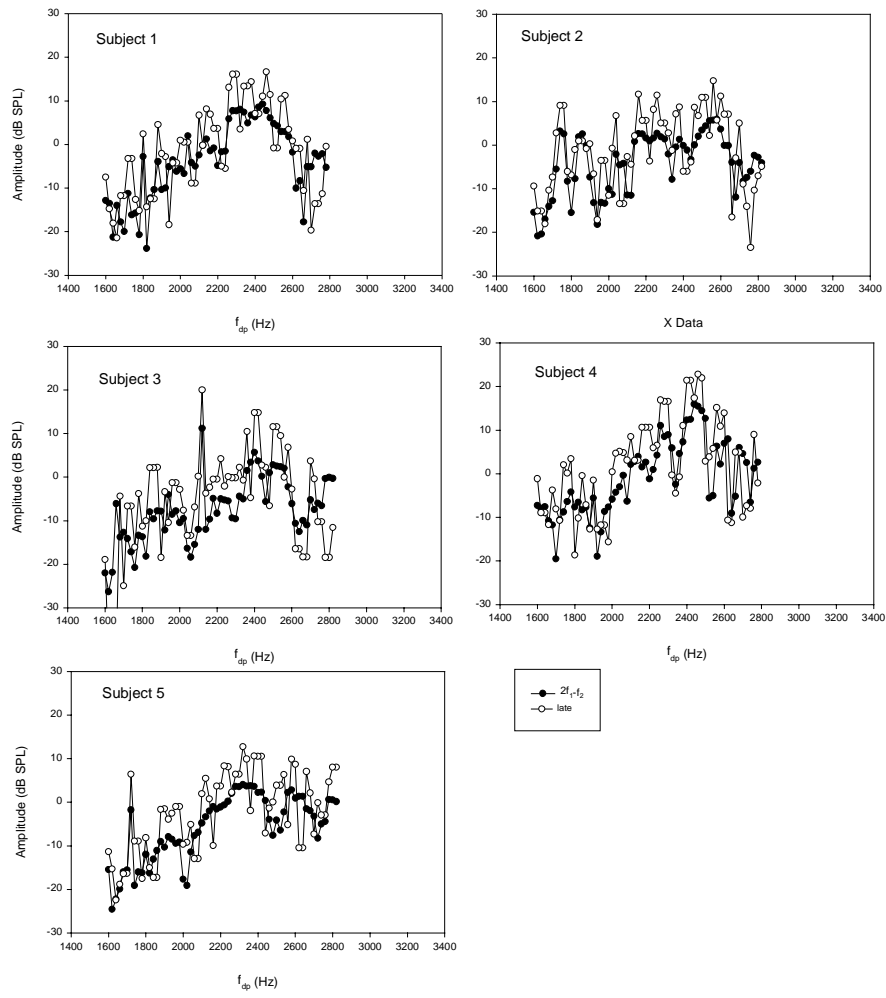


**Figure 17: The amplitude of the complete  $2f_1-f_2$  DPOAE and its late component using the  $f_1$  fixed at 3000 Hz protocol is plotted as a function of  $f_{dp}$  for the first measurement. The solid dot represents the complete  $2f_1-f_2$  DPOAE. The circle represents the late component. Data for each subject are shown in separate panel.**

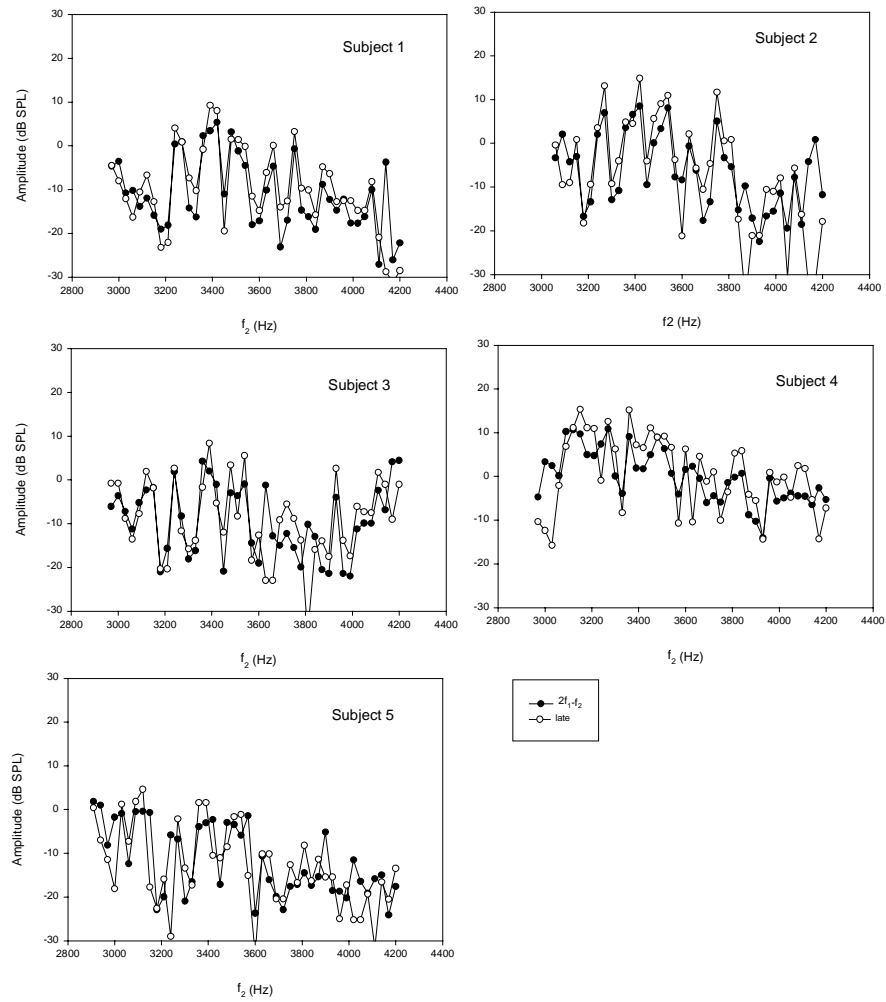


**Figure 18: Amplitude of the complete  $2f_1-f_2$  DPOAE and its late component using the  $f_1$  fixed at 2800 Hz protocol is plotted as a function of  $f_2$  for the first measurement. The solid dot represents the complete  $2f_1-f_2$  DPOAE. The circle represents the late component. Data for each subject are shown in separate panel.**

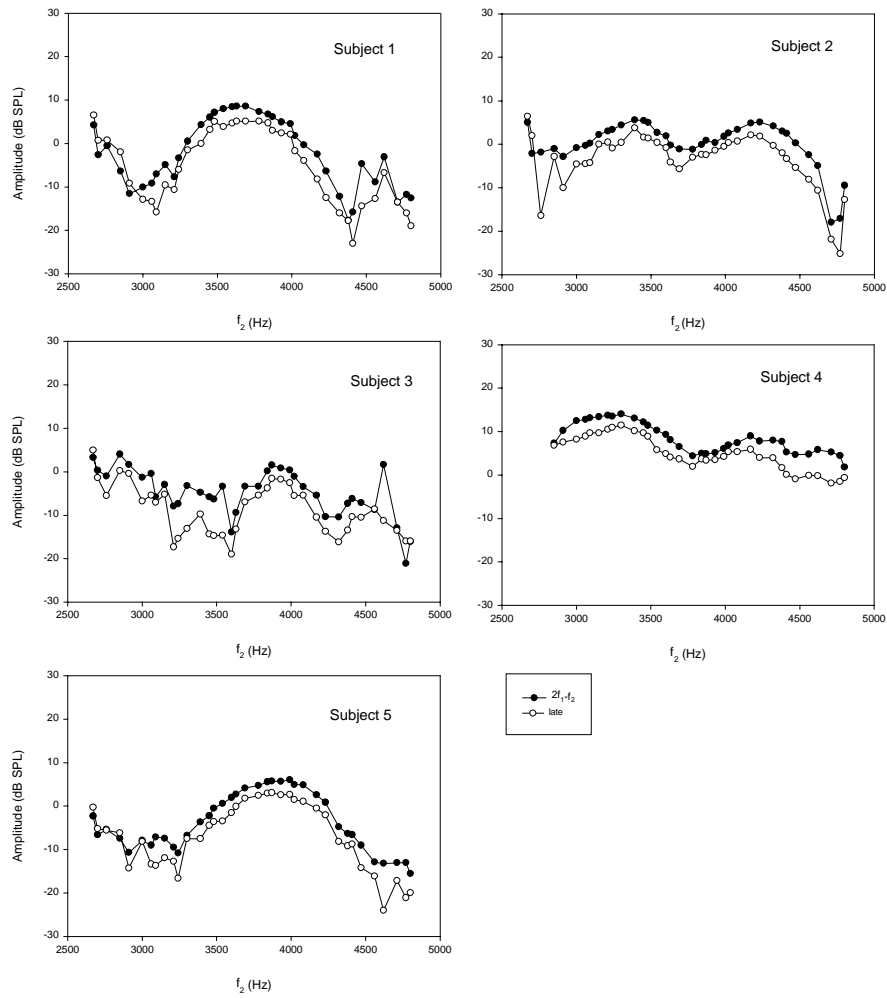
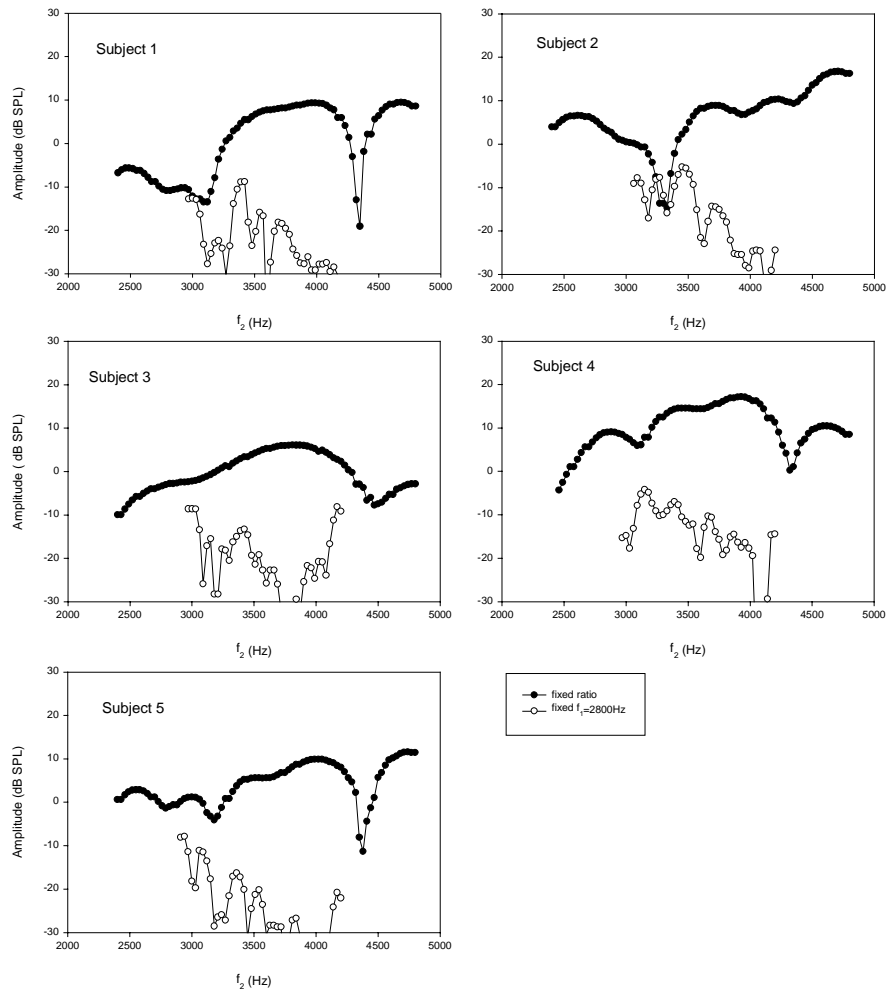


**Figure 19: Amplitude of the complete  $2f_1 - f_2$  DPOAE and its late components using the fixed  $f_{dp}$  protocol is plotted as a function of  $f_2$  for the first measurement. The solid dot represents the complete  $2f_1 - f_2$  DPOAE. The circle represents the late component. Data for each subject are shown in separate panel.**

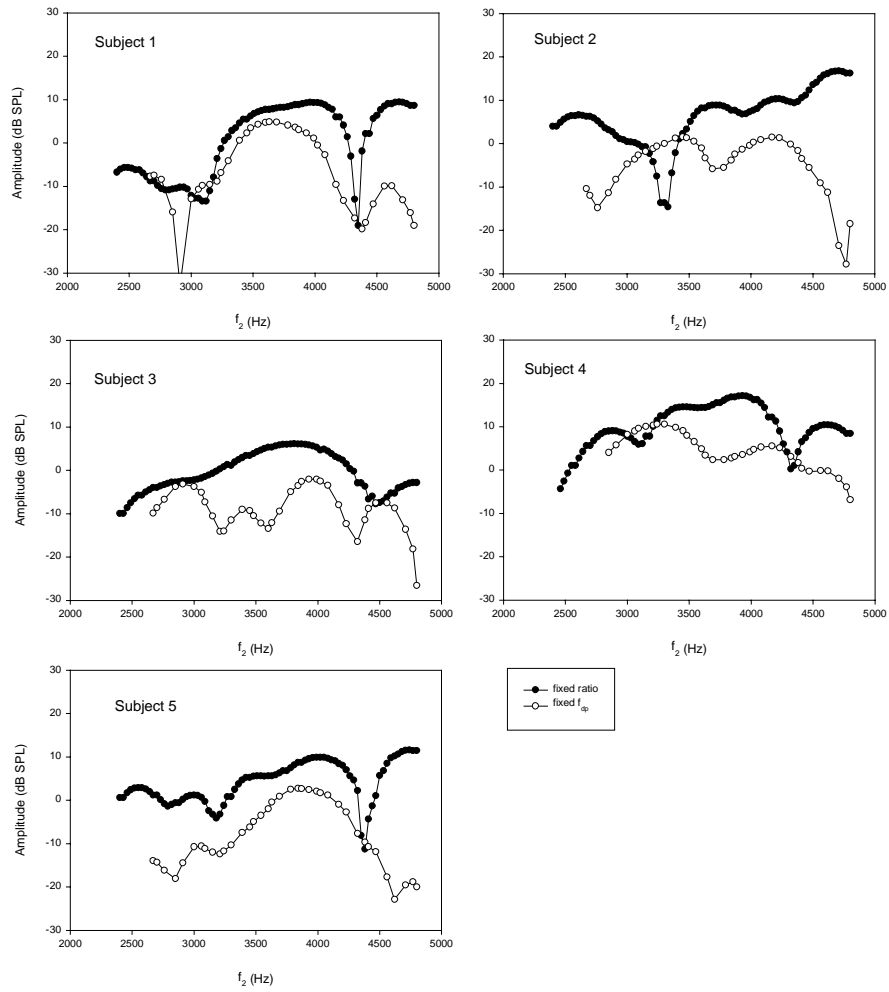
subjects. Both protocols produce smooth early component amplitude but they are the same pattern. The amplitude component amplitude of early component for the fixed  $f_2/f_1$  ratio protocol is much smoother than that for the  $f_1$  fixed at 2800 Hz protocol for all five subjects.

Figure 21 compares the early component amplitude for the fixed  $f_2/f_1$  ratio protocol and the fixed  $f_{dp}$  protocol for all five subjects. These early component amplitudes show smooth patterns, but again they are not the same. These early components represent cochlear response in the region of  $f_2$  for the same  $f_2$  frequency range (2400 Hz to 4800 Hz). The fixed or varied  $f_2/f_1$  ratio affects the amplitude of the emissions since the early components are “wave-fixed” emission. These within-subject comparisons have similar smooth pattern with essentially no fine structure, but they are not similar in shape due to the difference in protocol.

Figure 22 compares the  $2f_1-f_2$  DPOAE late component fine structure as a function of  $f_{dp}$  for the fixed  $f_2/f_1$  ratio protocol and the fixed  $f_2$  protocol for all five subjects. Figure 23 compares the  $2f_1-f_2$  DPOAE late component fine structure for the fixed  $f_2/f_1$  ratio protocol and the  $f_1$  fixed at 3000 Hz protocol. These late component fine structure represent the cochlear irregularities at the characteristic  $f_{dp}$  place for the same  $f_{dp}$  frequency range (1600 Hz to 3200 Hz), which results from the linear reflection and is a “place-fixed” emission. Each pair of these fine structures shows the similar high degree fine structure patterns for all five subjects.



**Figure 20:** The comparison of the amplitude of the early components between the fixed  $f_2/f_1$  ratio and the  $f_1$  fixed at 2800 Hz protocols is plotted as a function of  $f_2$  for the first measurement. The solid dot represents fixed  $f_2/f_1$  ratio protocol. The circle represents the  $f_1$  fixed at 2800 Hz protocol. Data for each subject are shown in separate panel.



**Figure 21: The comparison of the amplitude of the early components between the fixed  $f_2/f_1$  ratio and fixed  $f_{dp}$  protocols is plotted as a function of  $f_2$  for the first measurement. The solid dot represents fixed  $f_2/f_1$  ratio protocol. The circle represents the fixed  $f_{dp}$  protocol. Data for each subject are shown in separate panel.**

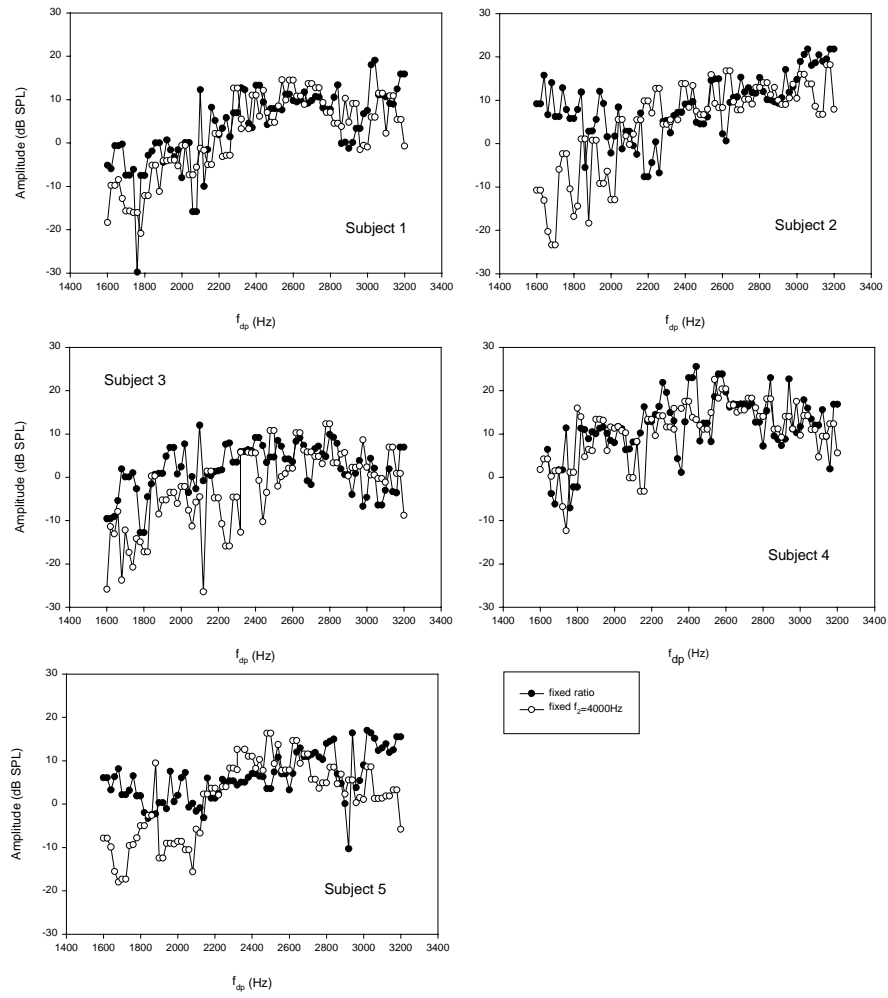


**Figure 22: The comparison of the late component fine structure between the fixed  $f_2/f_1$  ratio and the fixed  $f_2$  protocol is plotted as a function of  $f_{dp}$  for the first measurement. The solid dot represents fixed  $f_2/f_1$  ratio protocol. The circle represents the  $f_2$  fixed at 4000 Hz protocol. Data for each subject are shown in separate panel.**

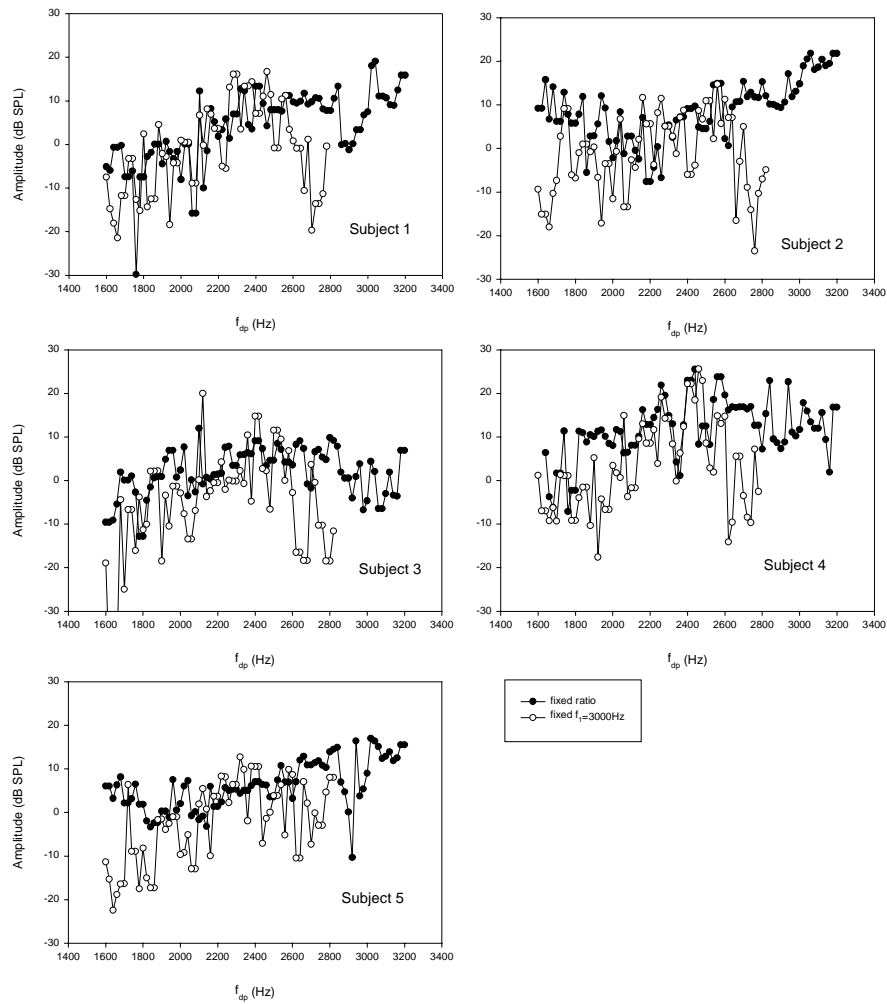


**Figure 23:** The comparison of the late component fine structure between the fixed  $f_2/f_1$  ratio and the  $f_1$  fixed at 3000 Hz protocols is plotted as a function of  $f_{ap}$  for the first measurement. The solid dot represents fixed  $f_2/f_1$  ratio protocol. The circle represents the  $f_1$  fixed at 3000 Hz protocol. Data for each subject are shown in separate panel.

## 5. Phase

The comparisons of the phase of the early versus the late components for the fixed  $f_2/f_1$  ratio, the  $f_1$  fixed at 2800 Hz, and fixed  $f_{dp}$  protocols were plotted as a function of  $f_2$  (Figure 24, 27, and 28). The comparisons of the phase of the early versus late component for the fixed  $f_2$  and the  $f_1$  fixed at 3000 Hz protocol were plotted as a function of  $f_{dp}$  (Figure 25 and 26). The phase of the DPOAE early component shows the same flat pattern for all five protocols from all five subjects. This is consistent with the hypothesis that this component is “wave-fixed” at the  $f_2$  place with a short latency. The phase of the DPOAE late components has the same pattern across subjects for each protocol. For the  $f_1$  fixed at 2800 Hz protocol the phase of DPOAE late component shows a “phase-lag” pattern for all five subjects. For the  $f_1$  fixed at 3000 Hz protocol the phase of the DPOAE late component shows a phase-lead pattern since it was plotted as a function of  $f_{dp}$ . This is expected because the  $f_{dp}$  place is moving apically (decreasing frequency) in the cochlea as  $f_2$  moves basally (increasing frequency) in this protocol. For the fixed  $f_2/f_1$  ratio, fixed  $f_2$ , and fixed  $f_{dp}$  protocols the phase of DPOAE late components show a “phase-lead” pattern for all five subjects.

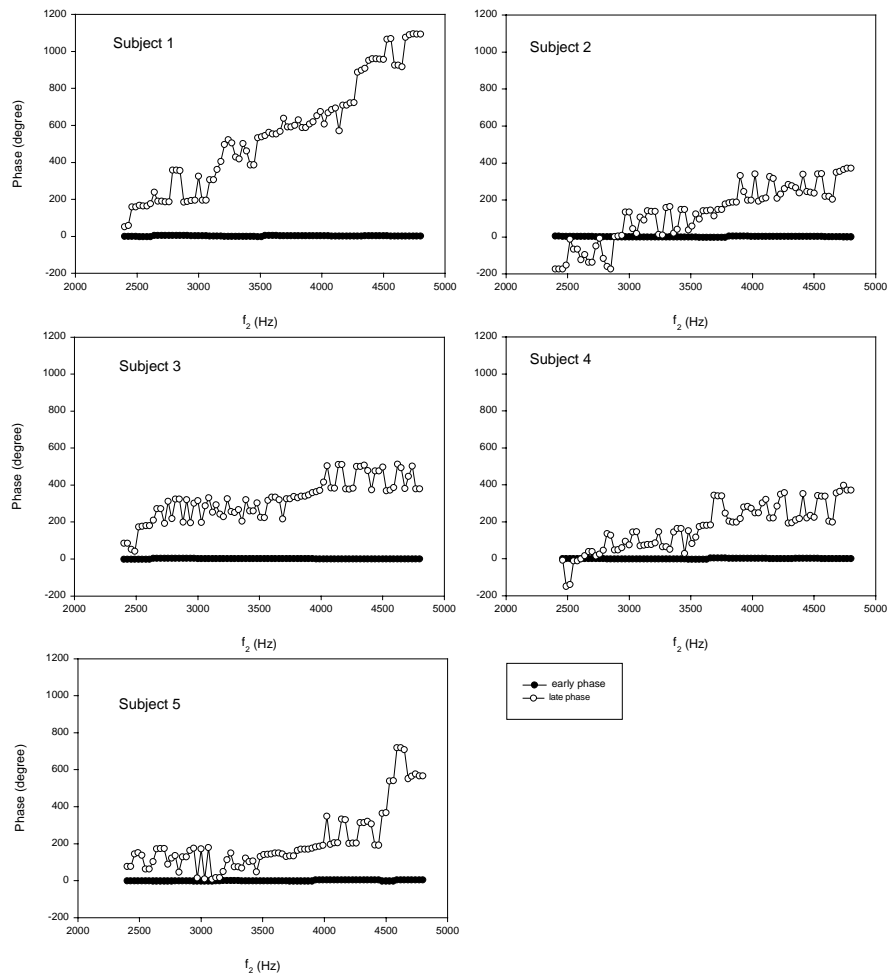


**Figure 24:** The unwrapped phase of the early and late components referred to the phase of the stimulus primary  $f_1$  using the fixed  $f_2/f_1$  ratio protocol is plotted as a function of  $f_2$  for the first measurement. The solid dot represents the phase of early component. The circle represents the phase of late component. Data for each subject are shown in separate panel.

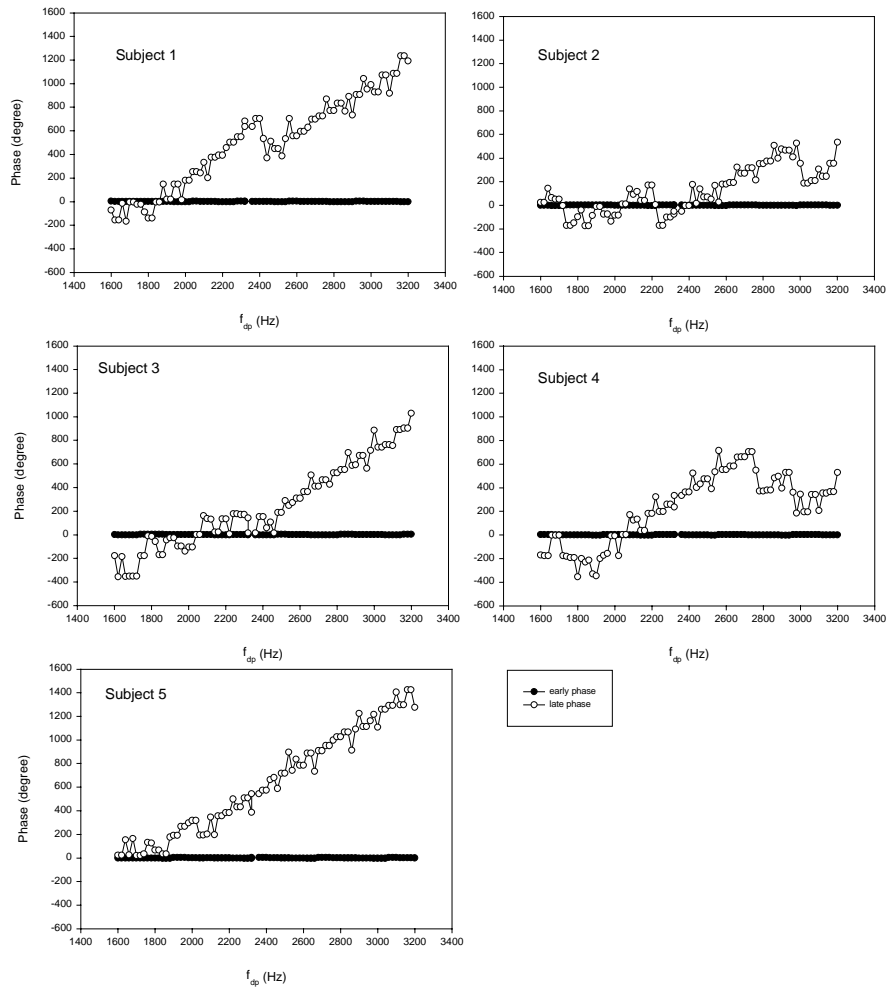


**Figure 25: The unwrapped phase of the early and late components referred to the phase of the stimulus primary  $f_1$  using the  $f_2$  fixed at 4000 Hz protocol is plotted as a function of  $f_{dp}$  for the first measurement. The solid dot represents the phase of early component. The circle represents the phase of late component. Data for each subject are shown in separate panel.**

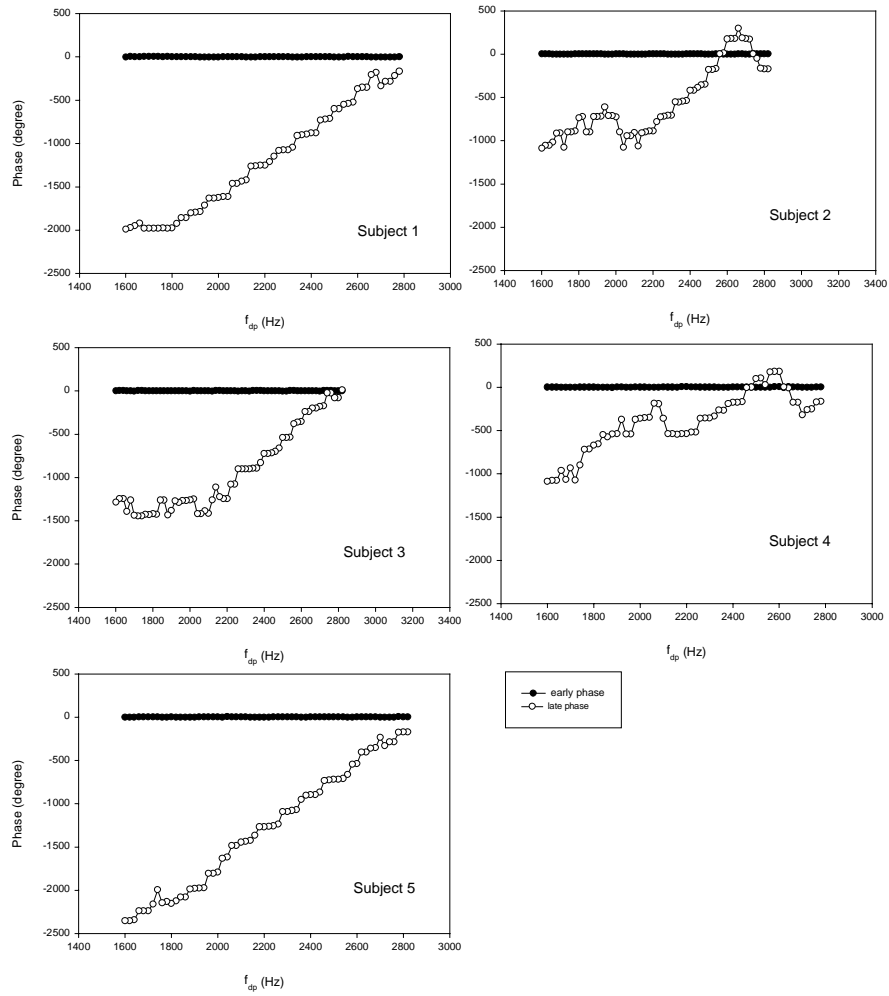


**Figure 26: The unwrapped phase of the early and late components referred to the phase of the stimulus primary  $f_1$  using the  $f_1$  fixed at 3000 Hz protocol is plotted as a function of  $f_{dp}$  for the first measurement. The solid dot represents the phase of early component. The circle represents the phase of late component. Data for each subject are shown in separate panel.**

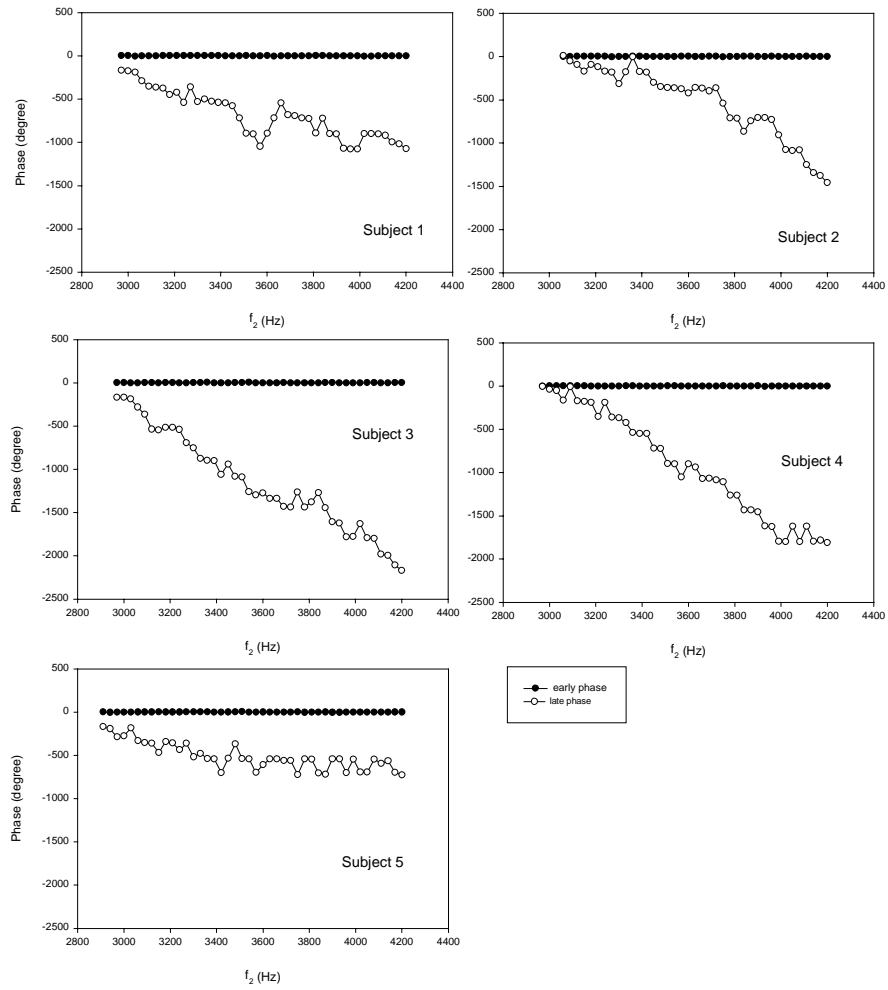


**Figure 27: The unwrapped phase of the early and late components referred to the phase of the stimulus primary  $f_1$  using the  $f_1$  fixed at 2800 Hz protocol is plotted as a function of  $f_2$  for the first measurement. The solid dot represents the phase of early component. The circle represents the phase of late component. Data for each subject are shown in separate panel.**

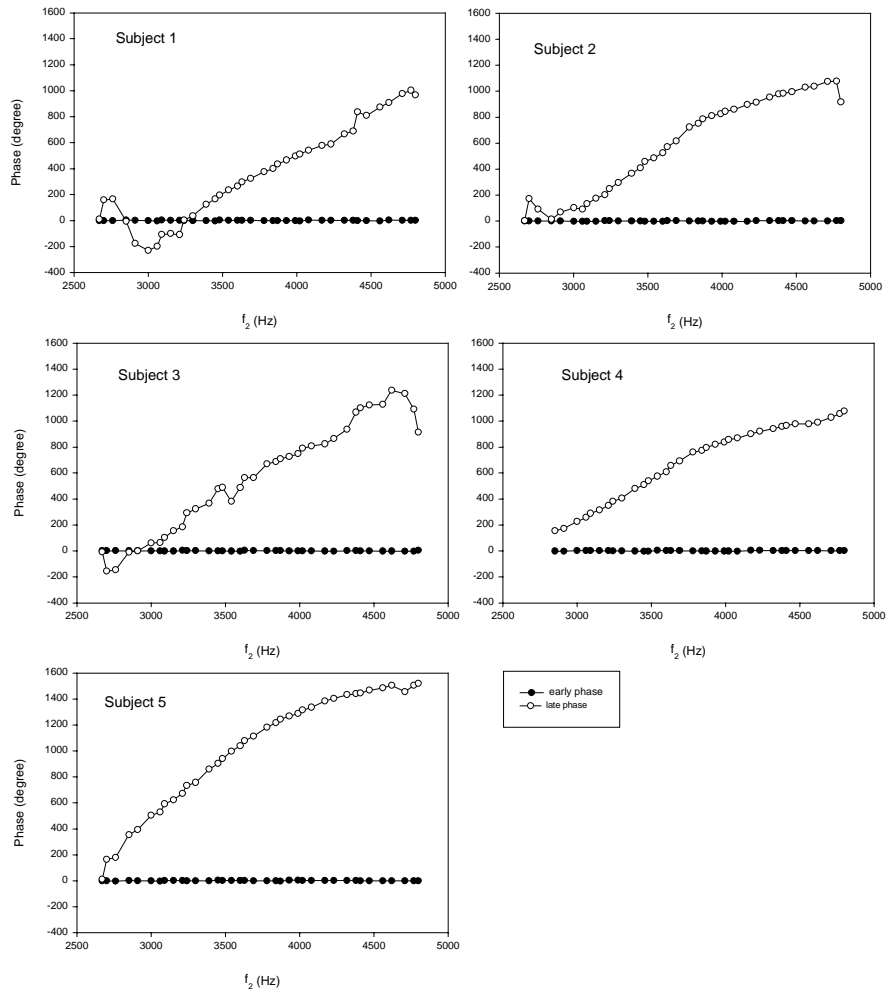


**Figure 28:** The unwrapped phase of the early and late components referred to the phase of the stimulus primary  $f_1$  using the fixed  $f_{dp}$  protocol is plotted as a function of  $f_2$  for the first measurement. The solid dot represents the phase of early component. The circle represents the phase of late component. Data for each subject are shown in separate panel.

## CHAPTER 4

### DISCUSSION

#### 4.1 Fine structure

The results obtained from this study show consistently small frequency space and great level difference fine structure using the fixed  $f_2/f_1$  ratio, the fixed  $f_2$ , the  $f_1$  fixed at 3000 Hz, and the  $f_1$  fixed at 2800 Hz protocols for all five subjects (Figure 5, 6, 7, and 8). These results indicate that the  $2f_1-f_2$  DPOAE fine structure can be obtained from normal hearing subjects as long as the linear reflection generation source ( $f_{dp}$  place) is not fixed at a particular place on the cochlear partition, regardless of the interference between the two generation sources. There are differences in the  $2f_1-f_2$  DPOAE fine structure patterns from subject to subject. These results are consistent with the previous studies.

If the DPOAE fine structure is dominated by the contribution from the characteristic place of the distortion product frequency, it is expected that the observable  $2f_1-f_2$  DPOAE pattern would show much less variation between minima and maxima when  $f_{dp}$  is held constant. Also the disappearance of fine structure during the fixed  $f_{dp}$  experiment shows that there is no coherent reflection from the primary region because there is no rotating phase with frequency (Mauermann et al,

1999). In this study, the DPOAEs obtained from all five subjects using the fixed  $f_{dp}$  protocol show a smooth and bandpass pattern (Figure 9). These results are consistent with previous studies (Mauermann et al 1999a, Piskorski 1997). The results support the  $f_{dp}$  place hypothesis that the DPOAE fine structure is dominated by the impedance property of the cochlear partition at the characteristic DP place. In other words, the characteristic DP place plays a major role for DPOAE fine structure. It is an only logical explanation for the origin of the DPOAE fine structure. When the DP place is held constant (the fixed  $f_{dp}$  protocol), the linear reflection portion of the emission is generated at the same place, a particular position on the basilar membrane. It indicates the same impedance property of the cochlear partition at the same characteristic cochlear partition place, so the DPOAE fine structure could not be obtained. When the DP place is moving along the cochlear partition (the fixed  $f_2/f_1$  ratio, fixed  $f_2$ , fixed  $f_1$  at 3000 Hz, and fixed  $f_1$  at 2800 Hz protocols), the linear reflection portion of the emission is generated along the cochlear partition. It represents a different impedance property at different characteristic DP positions along the cochlear partition, so DPOAE fine structure can be obtained from normal hearing subjects.

#### 4.2 Early and late components

It has been suggested that the two emission components are not simply arising from two distinct locations, but more importantly via two different mechanisms. (Kaulluri and Shera, 2000) The early component of DPOAEs, the so-called

distortion-source OAE depends upon the nonlinear interaction between the two primary traveling waves. The late component of DPOAEs, the so-called reflection-source emission, is generated when a forward-traveling wave reflects from local perturbations in the mechanics of the cochlea. In this study, the same patterns of the separated early and late components using the fixed  $f_2/f_1$  ratio, the fixed  $f_2$ , the  $f_1$  fixed at 3000 Hz, the  $f_1$  fixed at 2800 Hz protocols (Figure 10, 11, 12, and 13) indicate the same mechanism underlying the DPOAE fine structure. The early components that are generated in the  $f_2$  region by the nonlinear interaction between the two primaries show less variation in magnitude (solid dots in Figure 10, 11, 12, and 13) and phase (solid dots in Figure 24, 25, 26, and 27). The underlying mechanism for this early component is “wave-fixed”, the emission moves with the traveling wave envelope as frequency is changed. The major contribution is the nonlinear interaction of two primaries rather than the local impedance properties of the cochlear partition (Kemp 1986). The DPOAE late components, which result from a linear reflection at  $f_{dp}$  place, show pronounced fine structure (circles in Figure 10, 11, 12 and 13) and rapidly changing phase (circles in Figure 24, 25, 26, and 27). The underlying mechanism for this late component is “place-fixed”; perhaps the impedance irregularity of the cochlear partition responds to different phases of the stimulus as its frequency changes. The major contribution is the local impedance properties of the cochlear partition at the particular distortion product frequency place (Kemp 1986).

The within-subject comparisons between the amplitude of complete  $2f_1-f_2$  DPOAEs and its separated late components using the first four protocols were made. The results show that the complete  $2f_1-f_2$  DPOAEs and its late components have similar fine structure patterns for all five subjects (Figure 15, 16, 17 and 18) in terms of frequency space and level difference. This is strong evidence to support the  $f_{dp}$  place hypothesis. That is, the local impedance property of the cochlear partition at the  $f_{dp}$  place dominates the DPOAE fine structure. The interference of the two DPOAE generation sources has certain influence on the DPOAE amplitude, especially at low or high  $f_2/f_1$  ratio. So the complete  $2f_1-f_2$  DPOAEs and its late components do not have identical fine structure pattern in terms of the amplitude. These results can not be explained by the interference hypothesis.

The smooth pattern of  $2f_1-f_2$  DPOAEs for the fixed  $f_{dp}$  protocol (Figure 9) obtained from this study for all five subjects is consistent with the results obtained by Piskorski (1997) & Mauermann (1999). The separated early and late components of  $2f_1-f_2$  DPOAE using the fixed  $f_{dp}$  protocol for all five subjects show smooth curves for both early and late components (Figure 14). The within-subject comparison between the amplitude of the complete  $2f_1-f_2$  DPOAE and its late components using the fixed  $f_{dp}$  protocol shows almost identical smooth pattern too. If the interference of the two DPOAE generation sources plays a major role in DPOAE fine structure, then fine structure is expected from the fixed  $f_{dp}$  protocol. When  $f_{dp}$  is fixed, the characteristic DP place at the cochlear partition is fixed. Since the emission generated at the  $f_{dp}$  place is due to the linear reflection of the forward traveling

waves, when the primaries moves, the phase at the characteristic reflection place changes. The backward traveling wave from the two generation sources will not always match each other. So although the early and late components of DPOAE for the fixed  $f_{dp}$  protocol have an almost identical smooth pattern, as the phase of the late component changes rapidly, the fine structure will be expected due to interference of the early and late components. These results are another solid evidence to support the  $f_{dp}$  place hypothesis that the DPOAE fine structure is determined by the local impedance property of the cochlear partition rather than the interference of the two DPOAE generation sources.

### 4.3 Comparisons

The early components of  $2f_1-f_2$  DPOAEs are “wave-fixed”. The place of this emission moves with the traveling wave of the two primaries. In this study, when the fixed  $f_2/f_1$  ratio, the  $f_1$  fixed at 2800 Hz, and fixed  $f_{dp}$  protocols were used, the early components of  $2f_1-f_2$  DPOAE were not expected to have the same  $2f_1-f_2$  DPOAE pattern for the same  $f_2$  frequency range. The DPOAE early components are not expected to have the same pattern using different protocols. When the fixed  $f_2/f_1$  ratio protocol was used, the distance between the two generation sources was constant on a logarithmic scale. Then, the interference between the two generation sources was constant across swept. When the  $f_1$  fixed at 2800 Hz and fixed  $f_{dp}$  protocols were used, the distance between the two generation sources were different. Then the interference between the two generation sources varied across the swept.

For the same tested  $f_2$  frequency range (2400 Hz to 4800 Hz) along the cochlear partition, these early components would have the same smooth pattern but different amplitude. The difference is due to the  $f_2/f_1$  ratio changes. The comparisons of early components of  $2f_1-f_2$  DPOAE between different protocols (the fixed  $f_2/f_1$  ratio, the  $f_1$  fixed at 2800 Hz and the fixed  $f_{dp}$  protocols) indicate that the early components of the DPOAEs are induced by the interaction of the two primaries. The place of these emissions moves with the traveling wave envelopes as the stimulus frequency changed. The early components obtained from the  $f_1$  fixed at 2800 Hz protocol show a little more variation than the early components obtained from the fixed  $f_2/f_1$  ratio and fixed  $f_{dp}$  protocols. The  $f_2/f_1$  ratio influences the  $2f_1-f_2$  DPOAE amplitude. The  $f_2/f_1$  ratio was changed from 1.02 to 1.5 with the tested  $f_2$  frequency range of 2850 Hz to 4200 Hz for the  $f_1$  fixed at 2800 Hz protocol. The  $f_2/f_1$  ratio was changed from 1.02 to 1.35 with tested  $f_2$  frequency range of 2400 Hz to 4800 Hz for the fixed  $f_{dp}$  protocol. The  $f_2/f_1$  ratio changed more rapidly for the fixed  $f_1$  at 2800 Hz protocol than for the fixed  $f_{dp}$  protocol. When the two primaries were too close to each other or too far apart, the two emissions, the nonlinear distortion near the  $f_2$  place and linear reflection at  $f_{dp}$  place, will cancel each other. The amplitude of DPOAEs exhibits a bandpass shape (Stover et al. 1999). These results support that the early component of DPOAE is caused by the interaction of the two primaries. When the test protocol changed, the pattern of the DPOAE changes. The emission place moves with the two primaries traveling wave envelopes.

According to the  $f_{dp}$  place hypothesis, when the fixed  $f_2/f_1$  ratio, fixed  $f_2$ , and  $f_1$  fixed at 3000 Hz protocols were used, similar late component fine structure patterns would be expected in terms of frequency space and level difference. These fine structures are caused by the cochlear irregularities at  $f_{dp}$  place. Constant (the fixed  $f_2/f_1$  ratio protocol) or varied (the fixed  $f_2$ , and  $f_1$  fixed at 3000 Hz protocols) interference were occurred between the two DPOAE generation sources for the same  $f_{dp}$  frequency (1600 Hz to 3200 Hz) range along the cochlear partition. The comparisons of late component fine structure (Figure 22 and 23) show that the same  $f_{dp}$  range (1600 Hz to 3200 Hz) under different protocols could generate similar fine structure patterns in terms of frequency space and level difference. These results indicate that the late components of the DPOAEs are mainly caused by the impedance properties of local cochlear partition. Regardless of the test protocol, similar fine structure patterns could be obtained as long as the particular DP frequency range is the same. This emission place is fixed perturbation place at the particular frequency position of the cochlear partition. The same  $f_{dp}$  region generated a similar DPOAE fine structure pattern for different test protocol. These results could explain why the DPOAE fine structure would disappear when a third tone is introduced near the  $f_{dp}$  frequency. This suppressor tone will suppress the linear reflection DPOAEs at  $f_{dp}$  place, then the smooth pattern DPOAE early components will be the total DPOAE response recorded in the ear canal.

#### 4.4 Phase

Reflection-source emissions are generated when a forward-traveling wave reflects perturbations in the mechanics of the cochlea. The phase of this emission depends on the phase of the forward-traveling wave at the DP location. Since the micro-mechanical impedance perturbations are fixed in space (unlike sources of nonlinear distortion, which move with the excitation pattern as the frequency change), the phase of the incident wave at each perturbation changes as the frequency of the forward-traveling wave is varied (Zweig & Shera, 1995). Consequently, OAEs generated by linear reflection manifest a phase that rotates rapidly with frequency. The “wave-fixed” emission, the DPOAE early component, generated near  $f_2$  place due to the interaction of the two primaries has nearly constant phase. The “place-fixed” emission, the DPOAE late component, generated at the characteristic DP place has rapidly changing phase. The unwrapped phases of DPOAE early and late components obtained from this study show that the phase of the DPOAE early component has consistent flat phase pattern and the phase of the DPOAE late component is rapidly changing. That is consistent with the hypothesis that this component is place-fixed at the  $f_{dp}$  place with a longer latency.

#### 4.5. Further research and limitations of this study

The previous studies (Gaskill and Brown, 1996; Harris and Brown, 1994; Heitmann et al., 1998; and Mauermann et al., 1999) indicated that the  $2f_1$ - $f_2$  DPOAE fine structure appears to be a more sensitive indicator of cochlear damage than

DPOAE level alone. The evaluation of fine structure could considerably improve the clinical use of DPOAEs for early identification of hearing loss more accurately, especially for infants and neonates population. The fixed  $f_2/f_1$  ratio protocol will be the best test protocol for the clinical application. This fixed  $f_2/f_1$  ratio protocol minimizes the  $f_2/f_1$  ratio influence and keeps the highest amplitude of  $2f_1-f_2$  DPOAE across test swept. However, the clinical interpretation of the  $2f_1-f_2$  DPOAEs is not usually based in the comprehensive understanding of the  $2f_1-f_2$  DPOAEs. The understanding about the two different mechanism generation sources and the primary origin of the  $2f_1-f_2$  DPOAEs should be the foundation of the clinical interpretation of the  $2f_1-f_2$  DPOAE fine structure, in terms of frequency selectivity and site of lesion. The aim of accurate clinical interpretation of  $2f_1-f_2$  DPOAE fine structure makes clarification of the origin of the  $2f_1-f_2$  DPOAE fine structure significantly important.

In order to reach the aim of accurate clinical interpretation of  $2f_1-f_1$  DPOAE fine structure in terms of frequency selectivity and site of lesion, further studies should be done. First, whether the impedance property along the cochlear partition has the same characteristic in infants and adults is unclear. An investigation about the similarity of the impedance property of the cochlear partition between the infants and adults is necessary. In other words, a similar fine structure study needs to be done for infants. Second, the relationship between the auditory fine structure or stimulus frequency otoacoustic emission and DPOAE fine structure should be investigated.

The possibility of the results that have been artificially affected by the signal processing method has been considered. The most important signal processing in this study is that the  $2f_1-f_2$  DPOAEs are separated into the early and late components. These processing steps are stated in methodology section and showed in Figure 2. When each component is transformed back to the frequency domain via a FFT after windowing through a rectangular gate function, the amplitude spectrum in the frequency domain will have series of peaks that die away gradually as frequency increases. Since the time window for separating the  $2f_1-f_2$  DPOAE early and late components are determined based on peaks of the time domain DPOAE amplitude for different test protocol and subject individually, width of ripples caused by rectangular gate function are different from test protocol to test protocol, subject to subject.

When the amplitude of the  $2f_1-f_2$  DPOAE early components were transformed back to frequency domain via a FFT after windowing through a rectangular gate function, the time windows were set up from 1.2 to 5 milliseconds (ms) accordingly. The width of the ripples of the separated DPOAE early component for each test protocol and subject ranges from 200 Hz to 833 Hz (Table 4). These ripples do not correspond to the notches which appeared on the separated  $2f_1-f_2$  DPOAEs early components (Table 5). This indicates that the rectangular gate function does not affect the separated amplitude of the  $2f_1-f_2$  DPOAE early components.

		Subject1	Subject 2	Subject 3	Subject 4	Subject 5
Fixed $f_2/f_1$ ratio	Windowing	2.0 ms	1.5 ms	1.4 ms	2.0 ms	2.0 ms
	Ripple	500 Hz	666 Hz	714 Hz	500 Hz	500 Hz
Fixed $f_2$	Windowing	2.0 ms	1.7 ms	2.0 ms	2.1 ms	2.5 ms
	Ripple	500 Hz	588 Hz	500 Hz	475 Hz	400 Hz
Fixed $f_1$ at 3000 Hz	Windowing	5.0 ms	5.0 ms	5.0 ms	5.0 ms	5.0 ms
	Ripple	200 Hz	200 Hz	200 Hz	200 Hz	200 Hz
Fixed $f_1$ at 2800 Hz	Windowing	5.0 ms	5.0 ms	5.0 ms	5.0 ms	5.0 ms
	Ripple	200 Hz	200 Hz	200 Hz	200 Hz	200 Hz
Fixed $f_{dp}$	Windowing	1.8 ms	1.6 ms	1.2 ms	1.5 ms	1.7 ms
	Ripple	555 Hz	625 Hz	833 Hz	666 Hz	588 Hz

**Table 4: The width of ripples, which cause by the rectangular gate function for each test protocol and each subject.**

		Subject1	Subject 2	Subject 3	Subject 4	Subject 5
Fixed $f_2/f_1$ ratio	Notch	1260 Hz	400 Hz	2000 Hz	1300 Hz	1200 Hz
	Ripple	500 Hz	666 Hz	714 Hz	500 Hz	500 Hz
Fixed $f_2$	Notch	1200 Hz	1320 Hz	1050 Hz	300 Hz	2100 Hz
	Ripple	500 Hz	588 Hz	500 Hz	475 Hz	400 Hz
Fixed $f_1$ at 3000 Hz	Notch	1020 Hz	680 Hz	400 Hz	600 Hz	430 Hz
	Ripple	200 Hz	200 Hz	200 Hz	200 Hz	200 Hz
Fixed $f_1$ at 2800 Hz	Notch	330 Hz	360 Hz	510 Hz	580 Hz	270 Hz
	Ripple	200 Hz	200 Hz	200 Hz	200 Hz	200 Hz
Fixed $f_{dp}$	Notch	1470 Hz	1200 Hz	720 Hz	950 Hz	1600 Hz
	Ripple	555 Hz	625 Hz	833 Hz	666 Hz	588 Hz

**Table 5: Comparison of the width of signal processing ripples and the width of notches in the amplitude of DPOAEs early components for each of the protocols and for each subject.**

When the amplitude of the  $2f_1-f_2$  DPOAE late components were transformed back to frequency domain, the time windows were set up from 45 ms to 48.8 ms accordingly. The width of the ripples of the separated  $2f_1-f_2$  DPOAE late components for each test protocol and subject are range of 21 Hz to 22 Hz due to wide time duration. This range is very close to the frequency increment step of the  $2f_1-f_2$  DPOAE at  $f_{dp}$  frequency. If these ripples affect the amplitude of the  $2f_1-f_2$  DPOAE late components, the  $2f_1-f_2$  DPOAE late component fine structure will be either decreases or increases depending on the phase of ripples and are not

predictable. The  $2f_1-f_2$  DPOAE late components obtained using the fixed  $f_{dp}$  protocol showed smooth pattern and no ripples across the swept. Since the rectangular gate function has been used for separating the  $2f_1-f_2$  DPOAE early and late components for all five test protocols, this is an evidence that the rectangular gate function does not affect the amplitude of the  $2f_1-f_2$  DPOAE late components. The results obtained from this study are not artificially affected by the signal processing method.

There are some other limitations for this study. First, all comparisons are made by plot and done by visual inspection. No statistical comparisons are available. If a statistical method or a mathematical model can be used to compare the DPOAE fine structure under different test protocol, the results will be more precise.

Second, the comparisons are made in term of DPOAE fine structure. In this study, there is some disagreement between the amplitude and the fine structure for part of subjects (Fig. 22 and 23). The amplitude of DPOAEs is assumed to be less important than DPOAE fine structure. Whether this assumption is true is not clear. A further might be able to clarify it. A comparison of DPOAE late component using different test protocols can be made among a large number of subjects. Whether the amplitude of the DPOAE late components agrees with the fine structure or not can be clarified.

Third, there are many other windowing methods. Whether the rectangular gate function is a best way to separate DPOAE early and late components is not clear. A

further study to compare different windowing methods separating the DPOAE early and late components may find the best way to separate DPOAE early and late components without artificial effect.

## CHAPTER 5

### CONCLUSION

The results of this study support the hypothesis that DPOAE fine structure is dominated by the local impedance property of the cochlear partition at the characteristic DP frequency place rather than by interference between the two DPOAE generation sources.

The  $2f_1-f_2$  DPOAE fine structure has similar fine structure pattern as its late components, which generated at the particular characteristic DP frequency place along the cochlear partition, under the same test protocol and the same test frequency range for the same individual subject. This indicated that the local impedance property of the cochlear partition at the characteristic DP frequency place dominate the DPOAE fine structure. The early components do not affect the pattern of the complete  $2f_1-f_2$  DPOAE fine structure.

The complete  $2f_1-f_2$  DPOAE, and its early and late components show the same smooth pattern, when  $f_{dp}$  was held constant. This fact indicates that when the particular characteristic DP place along the cochlear partition is held unchanged cross the test frequency range, the DPOAE late components will be generated at the

same place and variations between the minima and maxima were not observed. Although the phase of the  $2f_1-f_2$  DPOAE late component still showed rapid change due to the primary generation source moving along the cochlear partition, no fine structure was obtained, regardless of interference between the two generation sources.

The  $2f_1-f_2$  DPOAE late components obtained from the same characteristic DP frequency under different test protocol showed the similar pattern of DPOAE fine structure regardless the same or different interference between the two DPOAE generation sources.

In conclusion, the test results of this experiment support the  $f_{dp}$  place hypothesis that the impedance property of the cochlear partition at the secondary DPOAE generation site, the particular characteristic  $f_{dp}$  place, rather than the interference of the two DPOAE generation sources dominate the DPOAE fine structure. Lack of the DPOAE fine structure may indicate a damage in particular proportion of cochlear partition. The  $f_{dp}$  place hypothesis will help clinical interoperation of DPOAE in terms of frequency selectivity and site of lesion.

**Appendix A**  
**Matlab program for calculating amplitude, phase of DPOAEs,**  
**and estimated noise floor from DPOAE time wave**

```

% main program to read biosig ascii files and calculate magnitude
% and phase of two primaries, three distortion products and three
noise
% floor estimates.

filename = input('Enter the filename of stored waveforms: ','s');

f1 = input('Enter the frequency of f1: ');
f2 = input('Enter the frequency of f2: ');
step1 = input('Enter the step size of f1: ');
step2 = input('Enter the step size of f2: ');
num = input('Enter the number of waveforms in the file: ');

[dpdata] = fileread(filename,num);
[mag,phase,fr] = calcul_fft(dpdata,f1,f2,step1,step2,num);

%calculate the noise floors
for j=1:num
    nfloor(j) = (mag(6,j) + mag(7,j) + mag(8,j))/3;
end

datname = input('Enter the name of the data file you want to write:
','s');

fdat = fopen(datname,'w');
for i=1:num

fprintf(fdat,'%8.4f,%8.4f,%8.4f,%8.4f,%8.4f,%8.4f,%8.4f,%8.4f,%8.4f,%8
.4f,%8.4f,%8.4f,%8.4f,%8.4f,%8.4f,%8.4f,%8.4f\n',...

mag(1,i),phase(1,i),fr(1,i),mag(2,i),phase(2,i),fr(2,i),mag(3,i),phase
(3,i),fr(3,i),mag(4,i),phase(4,i),...
    fr(4,i),mag(5,i),phase(5,i),fr(5,i),nfloor(i));
end
fclose(fdat);

```

**Appendix B**  
**Matlab program for computing the inverse FFT of DPOAE data**  
**(the time domain of the DPOAE amplitude across test protocol)**  
**and transform DPOAE early and late components back**  
**to frequency domain via FFT**

```

%program to compute the inverse FFT of dpoae data
%first find and read the data
files = input('How many data files do you want to read? ');
tot = 1;
for i = 1:files
    filename = input('Name of file?: ','s');
    num = input('How may waveforms in this file?');
    flread = zeros(num,16);
    flread = dlmread(filename,',' );
    data(tot:(tot+num-1),:) = flread; %data is the array for the
complete set of data from 2-3 data files
    tot = tot+num;
end
tot = tot-1; %the total number of waveforms in the dataset
%identify the specific columns of data
f2freq = data(:,6);
dp1freq = data(:,9);
dp1mag = data(:,7);
dp1ph = data(:,8);
%Magnitude data put back into linear form from SPL
dp1mag = 10.^(dp1mag/20) * 0.02;
cmpx1 = zeros(4096,1); %create cmpx1 data array and fill with 0s
%index for dpoae information into cmpx1 array
scale = input('As function of fdp or f2?:(1/2)');
while scale ~= 1 & scale ~= 2
    scale = input('You must answer 1 or 2. ');
end
switch scale
    case 2
        fi = round(f2freq/(25000/4096));
    case 1
        fi = round(dp1freq/(25000/4096));
end
%convert magnitude and phase data into cmpx1 data
for b=1:tot
    x = dp1mag(b) * cos(dp1ph(b) * pi/180);
    y = dp1mag(b) * sin(dp1ph(b) * pi/180);
    cmpx1(fi(b)) = x + (y*i);
end
%interpolate data between points

```

```

for i=2:tot
    diff = (fi(i) - fi(i-1));
    for n=1:diff
        cmpx1(fi(i)-n) = cmpx1(fi(i)) - n*(cmpx1(fi(i)) - cmpx1(fi(i-
1)))/diff;
    end
    %ramp up and down to and from beginning and end of signal
    end
    upramp = cmpx1(fi(1))/10;
    downramp = cmpx1(fi(tot))/10;
    for i=1:10
        cmpx1(fi(1)-i) = cmpx1(fi(1)) - (i * upramp);
        cmpx1(fi(tot)+i) = cmpx1(fi(tot)) - (i * downramp);
    end
    %perform the ifft
    impres = ifft(cmpx1);
    %write latency domain data to file
    yn = input('Do you want to separate the waveform now?y/n','s');
    if yn == 'y'
        cut = input('Where do you want to make separation?(msec)');
        cut = cut/0.02;
        short = zeros(4096,1);
        long = zeros(4096,1);
        short(1:cut) = impres(1:cut);
        long(cut:4096) = impres(cut:4096);
        shrt= fft(short);
        lng = fft(long);
        smoth = abs(shrt);
        micro = abs(lng);
        fast = angle(shrt);
        slow = angle(lng)* 360/(2*pi);
        lsmth = 20*log10(smoth/0.02);
        lmicr = 20*log10(micro/0.02);
        psmth = lsmth(fi);
        mic = lmicr(fi);
        flat = fast(fi);
        slat = slow(fi);
        filename = input('What is the name of the file for early
latency magnitude?','s');
        outfile = fopen(filename,'w');
        fprintf(outfile,'%g\n',psmth);
        fclose(outfile);
        filename = input('What is the name of the file for early latency
phase?','s');
        outfile = fopen(filename,'w');
        fprintf(outfile,'%g\n',flat);
        fclose(outfile);
        filename = input('What is the name of the file for later
latency magnitude?','s');
        outfile = fopen(filename,'w');
        fprintf(outfile,'%g\n',mic);
        fclose(outfile);
        filename = input('What is the name of the file for later
latency phase?','s');

```

```
        outfile = fopen(filename,'w');  
        fprintf(outfile,'%g\n',slat);  
    fclose(outfile);  
end
```

## Appendix C

### Matlab program for phase unwrapping

```
%routine to read data files and unwrap phase data
files = input('How many data files do you want to read? ');
tot = 1;
for i = 1:files
filename = input('What is the name of a file? ','s');
num = input('How may waveforms in this file?');
data = zeros(num,16);
data = dlmread(filename,',' );
phase(tot:(tot+num-1)) = data(:,8);
f1(tot:(tot+num-1)) = data(:,3);
f2(tot:(tot+num-1)) = data(:,6);
fdp(tot:(tot+num-1)) = data(:,9);
tot = tot+num;
end
phase = phase/(360/(2*pi));
newphase = unwrap(phase);
%newphase = phase;
%for i=2:tot-1
%   diff = abs(newphase(i-1) - phase(i));
%   while diff >= 180
%       newphase(i) = newphase(i) - 360;
%       newdiff = abs(newphase(i-1) - newphase(i));
%       if newdiff > diff
%           newphase(i) = newphase(i) + 360;
%           diff = 0;
%       else
%           diff = newdiff;
%       end
%   end
%end
newphase = newphase*(360/(2*pi));
phase = phase*(360/(2*pi));
newdata = zeros(5,(tot-1));
newdata(1,:) = f1;
newdata(2,:) = f2;
newdata(3,:) = fdp;
newdata(4,:) = newphase;
newdata(5,:) = phase;
size(newdata);
filename = input('What is the name of the file you want to
write?','s');
filedat = fopen(filename,'w');
```

```

fprintf(filedat,'%f, %f, %f, %f, %f\n',newdata);
fclose(filedat);

%routine to read data files and unwrap phase data
filename = input('What is the name of the file? ','s');
data = fopen(filename,'r');
num = input('How may waveforms in this file?');
phase = zeros(num);
phase = fscanf(data,'%g');
status = fclose(data);
phase = phase/(360/(2*pi));
newphase = unwrap(phase);
%newphase = phase;
%for i=2:tot-1
%   diff = abs(newphase(i-1) - phase(i));
%   while diff >= 180
%       newphase(i) = newphase(i) - 360;
%       newdiff = abs(newphase(i-1) - newphase(i));
%       if newdiff > diff
%           newphase(i) = newphase(i) + 360;
%           diff = 0;
%       else
%           diff = newdiff;
%       end
%   end
%end
newphase = newphase*(360/(2*pi));
phase = phase*(360/(2*pi));
filename = input('What is the name of the file you want to
write?','s');
filedat = fopen(filename,'w');
fprintf(filedat,'%f\n',newphase);
fclose(filedat);

```

## Bibliography

1. Avan P, Wit HP, Guitton M, Bonfils P (2000) On the spectral periodicity of transient-evoked otoacoustic emissions from normal and damaged cochleas Journal of Acoustical Society of America 108(3) 1117-1127
2. Brown AM, Kemp DT (1983) Otoacoustic emissions: the iso-suppression tuning properties of the distortion product  $2f_1-f_2$  in gerbil and man British Journal of Audiology 17 123-124
3. Brown AM, Kemp DT (1984) Suppressibility of the  $2f_1-f_2$  stimulated acoustic emissions in gerbil and men Hearing Research 13, 29-37
4. Brown AM, McDowell B, Forge A (1989) Acoustic distortion products can be used to monitor the effect of chronic Gentamycin treatment Hearing Research 42 143-156
5. Brown AM, Gaskill SA (1990) Measurement of acoustic distortion reveals underlying similarities between human and rodent mechanical responses Journal of Acoustical Society of America 88: 840-849
6. Brown AM, Harris FP, Beveridge HA (1996) Two sources of acoustic distortion products from the human cochlea Journal of Acoustical Society of America 100: (5) 3260-3267
7. Dallos P, Schoeny ZG, Worthington DW, Cheatham MA (1969) Some problems in the measurement of cochlear distortion Journal of Acoustical Society of America 46: 356-361
8. Davis H, (1983) An active process in cochlear mechanics. Hearing Research 9, 79-90
9. Furst M, Rabinowitz WM, Zurek PM (1988) Ear canal acoustic distortion at  $2f_1-f_2$  from human ears: Relation to other emissions and perceived combination tones Journal of Acoustical Society of America 84(1): 215-221

10. Gaskill SA, Brown AM (1990) The behavior of the acoustic distortion product,  $2f_1-f_2$ , from the human ear and its relation to auditory sensitivity Journal of Acoustical Society of America 88: 821-839
11. Gaskill SA, Brown AM (1996) Suppression of human acoustic distortion product: Dual origin of  $2f_1-f_2$  Journal of Acoustical Society of America 100(5): 3268-3273
12. Goldstein JL (1967) Auditory nonlinearity Journal of Acoustical Society of America 41:676-689
13. Harris FP, Lonsbury-Martin BL, Stager BB, Coats AC, Martin GK (1989) Acoustic distortion products in humans, systematic changes in amplitude as a function of  $f_2/f_1$  ratio Journal of Acoustical Society of America 85: 220-229
14. Harris FP, Brown AM (1994) Association of stimulus frequency and distortion product otoacoustic emission fine structure in human ears British Journal of Audiology 29 66
15. He N, Schmiedt RA (1993) Fine structure of  $2f_1-f_2$  distortion product emissions: changes with primary level Journal of Acoustical Society of America 94 2659-2669
16. He N, Schmiedt RA (1996) Fine structure of the  $2f_1-f_2$  acoustic distortion products: Effects of primary level and frequency ratios Journal of Acoustical Society of America 101 3554-3565
17. Heitmann J, Waldmann B, Schnitzler HU (1998) Suppression of distortion product otoacoustic emissions (DPOAE) near  $2f_1-f_2$  removes DP-gram fine structure-Evidence for a secondary generator Journal of Acoustical Society of America 103(3): 1527-1531
18. Iwasa KH, Chadwick RS (1992) Elasticity and force generation of cochlear outer hair cells Journal of Acoustical Society of America 92, 3169-3173
19. Kalluri R, Shera CA (2001) Distortion-product source unmixing: A test of two-mechanism model for DPOAE generation Journal of Acoustical society of America 109(2): 622-637
20. Kemp DT (1979) The evoked cochlear mechanical response and the auditory microstructure-evidence for a new element in cochlear mechanics Scand. Audiolol. Suppl. 9, 35-47
21. Kemp DT (1979) Evidence of mechanical nonlinearity and frequency selective wave amplification in the cochlea Arch. Otorhinolaryngol. 224: 37-45

22. Kemp DT, Brown AM (1983) An integrated view of cochlear mechanical nonlinearities observable from the ear canal Cochlea Mechanics pp 75-82
23. Kemp DT, Brown AM (1984) Ear canal acoustic and round window electrical correlations of  $2f_1-f_2$  distortion generated in the cochlea Hearing Research 13, 39-46
24. Kemp DT (1986) Otoacoustic emissions, travelling waves and cochlear mechanisms Hearing Research 22, 95-104
25. Kimberley BP, Brown DK, and Eggermont (1993) Measuring human cochlear traveling wave delay using distortion product emission phase responses Journal of the acoustical society of America 94: (3) 1343-1350
26. Knight RD, Kemp DT (2000) Indications of different distortion product otoacoustic emission mechanisms from a detailed  $f_1$ ,  $f_2$  area study Journal of the acoustical society of America 107: (1) 457-473
27. Knight RD, Kemp DT (2001) Wave and place fixed DPOAE maps of the human ear Journal of the Acoustical Society of America 109: (4) 1513-1525
28. Konrad-Martin D, Neely ST, Keefe DH, Dorn PA, Corga MP (2001) Sources of distortion product otoacoustic emissions revealed by suppression experiments and inverse fast Fourier transforms in normal ears Journal of Acoustical Society of America 109: (6) 2862-2879
29. Long G (1984) The microstructure of quiet and masked thresholds Hearing Research 15 73-87
30. Manley GA Frequency spacing of acoustic emissions: A possible explanation Mechanisms of Hearing, edited by Webster WR & Aitken LM pp. 36-39
31. Mauermann M, Uppenkamp S, van Hengel PWJ, Kollmeier B (1999a) Evidence for the distortion product frequency place as a source of distortion product otoacoustic emission (DPOAE) fine structure in humans. I. Fine structure and higher-order DPOAE as a function of the frequency ratio  $f_2/f_1$  Journal of the acoustical society of America 106: (6) 3473-3483
32. Mauermann M, Uppenkamp S, Van Hengel PWJ, Kollmeier B (1999b) Evidence for the distortion product frequency place as a source of distortion product otoacoustic emission (DPOAE) fine structure in humans. II. Fine structure for different shapes of cochlear hearing loss Journal of the acoustical society of America 106: (6) 3484-3491

33. Moulin A, Kemp DT, Multicomponent acoustic distortion product otoacoustic emission phase in humans. I. General characteristics Journal of Acoustical Society of America 100 (3) 1617-1639
34. Piskorski, P. (1997) The origin of the distortion product otoacoustic emission fine structure Ph. D. Thesis, Purdue University, West Lafayette, IN
35. Probst R, Lonsbury BL, Martin GK (1990) A review of otoacoustic emissions Journal of Acoustical Society of America 89:( 5) 2027-2067
36. Rhode WW (1971) Observations of the vibrations of the basilar membrane in squirrel monkeys using the Mossbauer technique. Journal of Acoustical Society of America 49: 1218-1231
37. Robles L, Ruggero MA, and Rich NC (1993) Distortion products at the basilar membrane of the cochlea: Dependence on stimulus frequency and intensity and effect of acoustic trauma Neuroscience Abstracts 19, 1421
38. Ruggero MA, Rich NC (1991) Application of a commercially manufactured Doppler shift laser velocimeter to the measurement of basilar membrane vibration Hearing Research 51, 215-230
39. Schloth E (1983) Relation between spectral composition of spontaneous otoacoustic emissions and fine structure of threshold in quiet Acustica 53: 250 256
40. Shera CA, Zweig G (1993) Noninvasive measurement of the cochlear traveling-wave ratio Journal of Acoustical Society of America 93: (6) 3333-3352
41. Shera CA, Guinan JJ, Jr (1999) Evoked otoacoustic emissions arise by two fundamentally different mechanisms: A taxonomy for mammalian OAEs Journal of Acoustical Society of America 105: (2) 782-798
42. Shera CA (2001) Intensity-invariance of fine time structure in basilar-membrane click responses: Implications for cochlear mechanics Journal of acoustical society of America 110: (1) 332-348
43. Smoorenburg GF (1972) Combination tone and their origin Journal of Acoustical Society of America 52: 615-632
44. Smoorenburg GF (1972) Audibility region of combination tones Journal of Acoustical Society of America 52: 603-614
45. Stover LJ, Norton SJ (1992) The effects of aging on otoacoustic emissions Journal of Acoustical Society of America 94: (5) 2670-2681

46. Stover LJ, Neely ST, Gorga MP (1996) Latency and multiple sources of distortion otoacoustic emissions Journal of Acoustical Society of America 99: 1016-1024
47. Stover LJ, Gorga MP, Neely ST (1996) Toward optimizing the clinical utility of distortion product otoacoustic emission measurements Journal of Acoustical Society of America 100: (2) 956-967
48. Stover LJ, Neely ST, Gorga MP (1999) Cochlear generation of intermodulation distortion revealed by DPOAE frequency functions in normal and impaired ears Journal of Acoustical Society of America 105:2669-2678
49. Sun XM, Schmiedt RA, He N, and Lam C. (1994) Modeling the fine structure of the  $2f_1-f_2$  acoustic distortion product. I. Model development Journal of Acoustical Society of America 96:2166-2174
50. Sun XM, Schmiedt RA, He N, and Lam C. (1994) Modeling the fine structure of the  $2f_1-f_2$  acoustic distortion product. II. Model evaluation Journal of Acoustical Society of America 96:2175-2183
51. Talmadge CL, Tubis A, Long GR (1998) Modeling otoacoustic emission and hearing threshold fine structures Journal of Acoustical Society of America 104: (3) 1517-1543
52. Talmadge CL, Long GR, Tubis A (1999) Experimental confirmation of the two-source interference model for the fine structure of distortion product otoacoustic emissions Journal of Acoustical Society of America 105:91) 275-292
53. Talmadge CL, Tubis A, Long GR, Tong C, (2000) Modeling the combined effects of basilar membrane nonlinearity and roughness on stimulus frequency otoacoustic emission structure Journal of Acoustical Society of America 108: (6) 2911-2932
54. Tubis A, Talmadge CL, Tong C, Dhar S (2000) On the relationships between the fixed- $f_1$ , fixed- $f_2$  and fixed-ratio phase derivatives of the  $2f_1-f_2$  distortion product otoacoustic emission Journal of Acoustical Society of America 108: (4) 1772-1785
55. Van Hengel PWJ, Duifhuis H, Van Den Raadt MPMG (1996) Spatial periodicity in the cochlea: the result of interaction of spontaneous emissions? Journal of Acoustical Society of America 99:3566-3571
56. Wilson JP (1980) Evidence for a cochlear origin for acoustic re-emissions, threshold fine structure and tonal tinnitus Hearing Research 2, 233-252

57. Wilson JP (1980) The combination tone  $2f_1-f_2$ , in psychophysics and ear canal recording in Psychophysical, Physiological, and Behavioral Studies in hearing edited by Van Den Brink G and Bilsen FA (Delft U.P., Delft, The Netherlands), pp. 43-50
58. Zweig G, Shera CA (1995) The origin of periodicity in the spectrum of evoked otoacoustic emission Journal of Acoustical Society of America 98: (4) 2018-2042
59. Zwicker E, Schloth E (1984) Interrelation of different oto-acoustic emissions Journal of Acoustical Society of America 75 (4) 1148-1154